ORIGINAL ARTICLE

Identification of Leading Compounds from *Euphorbia neriifolia* (Dudsor) Extracts as a Potential Inhibitor of SARS-CoV-2 ACE2-RBDS1 Receptor Complex: An Insight from Molecular Docking ADMET Profiling and MD-simulation Studies

Md Nur Islam[1], Md Enayet Ali Pramanik[2], Md Arju Hossain[3], Md Hasanur Rahman[4], Md Sahadot Hossen[5], Md Ashraful Islam[6], M Morsed Zaman Miah[7], Istiak Ahmed[8], AZM Mostaque Hossain[9], Md Jawadul Haque[10], AKM Monoarul Islam[11], Md Nowshad Ali[12], Rukhshana Akhter Jahan[13], Md Enamul Haque[14], Md Munzur Rahman[15], Md Sharif Hasan[16], Mohammad Motiur Rahman[17], Md Mamun Kabir[18], Prabir Mohan Basak[19], Md Abdul Mumit Sarkar[20], Md Shafiqul Islam[21], Md Rashedur Rahman[22], AKM Azad-ud-doula Prodhan[23], Ashik Mosaddik[24], Humayra Haque[25], Fahmida Fahmin[26], Haimanti Shukla Das[27], Md Manzurul Islam[28], Chandrima Emtia[29], Md Royhan Gofur[30], Aiping Liang[31], Sheikh Mohammad Fazle Akbar[32]

Received on: 21 October 2023; *Accepted on*: 23 November 2023; *Published on*: 22 December 2023

Abstract

Coronavirus disease-19 (COVID-19) are deadly and infectious disease that impacts individuals in a variety of ways. Scientists have stepped up their attempts to find an antiviral drug that targets the spike protein (S) of Angiotensin converting enzyme 2 (ACE2) (receptor protein) as a viable therapeutic target for coronavirus. The most recent study examines the potential antagonistic effects of 17 phytochemicals present in the plant extraction of *Euphorbia neriifolia* on the anti-SARS-CoV-2 ACE2 protein. Computational techniques like molecular docking, absorption, distribution, metabolism, excretion, and toxicity (ADMET) investigations, and molecular dynamics (MD) simulation analysis were used to investigate the actions of these phytochemicals. The results of molecular docking studies showed that the control ligand (2-acetamido-2-deoxy-β-D-glucopyranose) had a binding potential of –6.2 kcal/mol, but the binding potentials of delphin, β-amyrin, and tulipanin are greater at –10.4, 10.0, and –9.6 kcal/mol. To verify their drug-likeness, the discovered hits were put via Lipinski filters and ADMET analysis. According to MD simulations of the complex run for 100 numbers, delphin binds to the SARS-CoV-2 ACE2 receptor's active region with good stability. In root-mean-square deviation (RMSD) and root mean square fluctuation (RMSF) calculations, delphinan, β-amyrin, and tulipanin showed reduced variance with the receptor binding domain subunit 1(RBD S1) ACE2 protein complex. The solvent accessible surface area (SASA), radius of gyration (Rg), molecular surface area (MolSA), and polar surface area (PSA) validation results for these three compounds were likewise encouraging. The convenient binding energies across the 100 numbers binding period were discovered by using molecular mechanics of generalized born and surface (MM/GBSA) to estimate the ligand-binding free energies to the protein receptor. All things considered, the information points to a greater likelihood of chemicals found in *Euphorbia neriifolia* binding to the SARS-CoV-2 ACE2 active site. To determine these lead compounds' anti-SARS-CoV-2 potential, in vitro and *in vivo* studies should be conducted.

Keywords: Absorption, distribution, metabolism, excretion, and toxicity (ADMET), Angiotensin converting enzyme 2, Coronavirus disease-19, *Euphorbia neriifolia* and phytochemicals, Molecular docking, Molecular dynamics simulation, Molecular mechanics of generalized born and surface.

Euroasian Journal of Hepato-Gastroenterology (2023): 10.5005/jp-journals-10018-1414

Introduction

Early in December 2019, Wuhan, China, reported that the respiratory disease known as "coronavirus disease-19 (COVID-19)" was caused by the Severe acute respiratory syndrome–related coronavirus 2 (SARS-CoV-2) that has since spread around the globe.[1] This dreadful virus has evolved as one of the most fatal human illnesses on earth since its first outbreak in China.[2] The 30 kb single-stranded positive-sense coronaviruses have a diameter of 65–125 nm.[3] The β-coronaviruses of the Coronaviridae family are enveloped RNA viruses that fall into five classes: α, β, γ, δ, and ο coronavirus.[4,5] Because of the disease's widespread distribution and severeness around the world, the World Health Organization (WHO) has designated it as a public health issue of worldwide concern (Fig. 1).[6,7] There is a correlation between age, smoking status, ethnicity, and male sex with SARS-CoV-2 infection.[8,9] It's interesting to note

[1]National Laboratory of Biomacromolecules, Chinese Academy of Sciences Center for Excellence in Biomacromolecules, Institute of Biophysics; University of Chinese Academy of Sciences, Beijing, People's Republic of China

[2,31]Key Laboratory of Zoological Systematics and Evolution, Institute of Zoology, College of Life Sciences, University of Chinese Academy of Sciences (UCAS), Beijing, People's Republic of China; On-Farm Research Division, Bangladesh Agricultural Research Institute, Rajshahi, Bangladesh

[3]Department of Biotechnology and Genetic Engineering, Mawlana Bhashani Science and Technology University, Santosh, Tangail, Bangladesh

[4]Department of Biotechnology and Genetic Engineering, Faculty of Life Sciences, Bangabandhu Sheikh Mujibur Rahman Science and Technology University (BSMRSTU), Gopalganj, Bangladesh

that patient age and underlying health issues affect COVID-19 persistence and prognosis.[10] The etiology of this sickness is SARS-CoV-2 infection, which induces hyperinflammation that increases alveolar permeability. This hyperinflammation leads to a quickly fatal hypercytokinemia with multiorgan failure, and angiotensin converting enzyme 2 (ACE2) enzyme activity is suppressed.[11,12]

Little is known about the human immune response to SARS-CoV-2 infection, despite mounting fears about the potentially catastrophic worldwide spread of COVID-19.[13,14] Severe acute respiratory syndrome–related coronavirus infections may spread to other people via the nasal epithelium. Recently, the use of *Euphorbia neriifolia* leaf juice in human trials has shown a significant improvement in COVID-19 illness recovery in Bangladesh.[15] The rate of viral replication and severity of the sickness are significantly impacted when the protein of SARS-S CoV-2 attaches to ACE2 as a receptor for cellular entrance).[14,16,17] A number of methods have been proposed to interfere with the SARS-CoV-2 protein S-ACE2 binding. The N501Y mutation shown in the RBD-S1 complex enhances the interaction in all strains of variants that have been found, including B117, P1351, and P1 in the UK, South Africa, and Brazil, respectively. In this instance, addressing the ACE2 receptor could be an alternative to focusing on RBD. The SARS-CoV-2 spike (S) protein plays a crucial role in the fusion of the host cell membrane with the viral membrane during infection.[18,19] When the receptor-binding domain (RBD) of ACE2 is linked to the peptidase domain (PD), host proteases that split the S1 and S2 subunits at their N and C terminals activate the S protein.[20,21] Scientists have previously raised concerns about the use of drugs that target the renin-angiotensin signaling (RAS) system.[22–24] Nonetheless, Jia et al. detailed the present efforts to target the ACE2 receptor for SARS-CoV-2 therapy (Fig. 1).[25]

The persisting SARS-CoV2 pandemic, as well as a lack of thorough understanding of the course of COVID-19, has limited our capacity to create effective therapies for afflicted individuals. However, blocking the SARS-CoV-2 protein S-ACE2 connection by targeting the ACE2 receptor might be a potential technique. In a recent study, the COVID-19 ο variation has prompted worldwide worry about altering vaccination programs and also slow vaccine rollout.[5] Furthermore, this critical situation makes patients psychologically discomfort; the resulting public health continues to be threatened by COVID-19.[26,27] Coronavirus disease-19 patients are solely eligible for curative and supportive care; also as infections continue to increase on a regular schedule, there is an immediate want for effective treatment medications. For this pure, several scientific organizations globally are now focused to identify new effective antiviral drugs utilizing bioinformatics approaches of different organic plants like tea, *Vernonia amygdalina*, neem (*Azadirachta indica*) and some phytochemicals including, kolaviron, apigenin, and fisetin.[28–31] During the 2003 SARS outbreak, the efficacy of a therapy based on traditional medicinal herbs was documented.[32]

Several potential phytochemicals found in *Euphorbia neriifolia* were tested for their ability to inhibit COVID-19 ACE2 protein complex (6VW1), investigated in our study. Native to India, *Euphorbia neriifolia* was scientifically proven to treat bronchitis, tumors, inflammation, and other diseases as well as to be hazardous to human beings.[33] It has been studied for several decades from a phytochemical perspective. Euphorbias have traditionally been used as a folk medicine to treat cough and asthma due to its anti-inflammatory, antibacterial, and antiparasitic characteristics.[34,35] Scientists think that natural chemicals originating from plants can protect against viral infection by functioning as therapeutic

[5]Department of Biochemistry and Molecular Biology, School of Life Sciences, Shahjalal University of Science and Technology, Sylhet, Bangladesh

[6]Department of Clinical Pharmacy, Imam Abdulrahman Bin Faisal University, Dammam, Saudi Arabia

[7]Department of Haematology, Rajshahi Medical College, Rajshahi, Bangladesh

[8,9]Department of Surgery, Rajshahi Medical College Hospital, Rajshahi, Bangladesh

[10]Department of Community Medicine, Rajshahi Medical College, Rajshahi, Bangladesh

[11]Department of Nephrology, Rajshahi Medical College, Rajshahi, Bangladesh

[12]Department of Pediatric Surgery, Rajshahi Medical College, Rajshahi, Bangladesh

[13]Department of Pathology, Rajshahi Medical College, Rajshahi, Bangladesh

[14,15]Department of Ortho-Surgery, Rajshahi Medical College, Rajshahi, Bangladesh

[16]Department of Cardiology, Mymensingh Medical College Hospital, Mymensingh, Bangladesh

[17–19]Department of Medicine, Rajshahi Medical College, Rajshahi, Bangladesh

[20,21]Department of Gastroenterology, Rajshahi Medical College, Rajshahi, Bangladesh

[22]Department of Agronomy, Bangladesh Agricultural University, Mymensingh, Bangladesh

[23]Department of Botany, Bangladesh Agricultural University, Mymensingh, Bangladesh

[24]Director, Center for Interdisciplinary Research, Varendra University, Rajshahi, Bangladesh

[25]Department of Anaesthesia, Analgesia & Intensive Care Unit, Chattogram Medical College, Chattogram, Bangladesh

[26]Department of Paediatric, Mymensingh Medical College Hospital, Mymensingh, Bangladesh

[27]Department of Virology, Rajshahi Medical College, Rajshahi, Bangladesh

[28]Director, Prime Minister Office and Private Secretary of Economic Advisor to the Hon'ble Prime Minister of Bangladesh, Prime Minister's Office, Tejgaon, Dhaka, Bangladesh

[29]Laboratory of Systems Ecology, Faculty of Agriculture, Saga University, Honjo, Saga, Japan

[30]Department of Veterinary and Animal Sciences, University of Rajshahi, Rajshahi, Bangladesh

[32]Department of Gastroenterology and Metabology, Ehime University Graduate School of Medicine; Research Center for Global and Local Infectious Diseases, Faculty of Medicine, Oita University, Oita; Miyakawa Memorial Research Foundation, Tokyo, Japan

Corresponding Author: Md Enayet Ali Pramanik, Key Laboratory of Zoological Systematics and Evolution, Institute of Zoology, College of Life Sciences, University of Chinese Academy of Sciences (UCAS), Beijing, People's Republic of China; On-Farm Research Division, Bangladesh Agricultural Research Institute, Rajshahi, Bangladesh, Phone: +01744530588, e-mail: enayet.bari.bd@gmail.com

How to cite this article: Islam MN, Pramanik MEA, Hossain MA, *et al*. Identification of Leading Compounds from *Euphorbia Neriifolia* (Dudsor) Extracts as a Potential Inhibitor of SARS-CoV-2 ACE2-RBDS1 Receptor Complex: An Insight from Molecular Docking ADMET Profiling and MD-simulation Studies. Euroasian J Hepato-Gastroenterol 2023;13(2):89–107.

Source of support: Nil

Conflict of interest: None

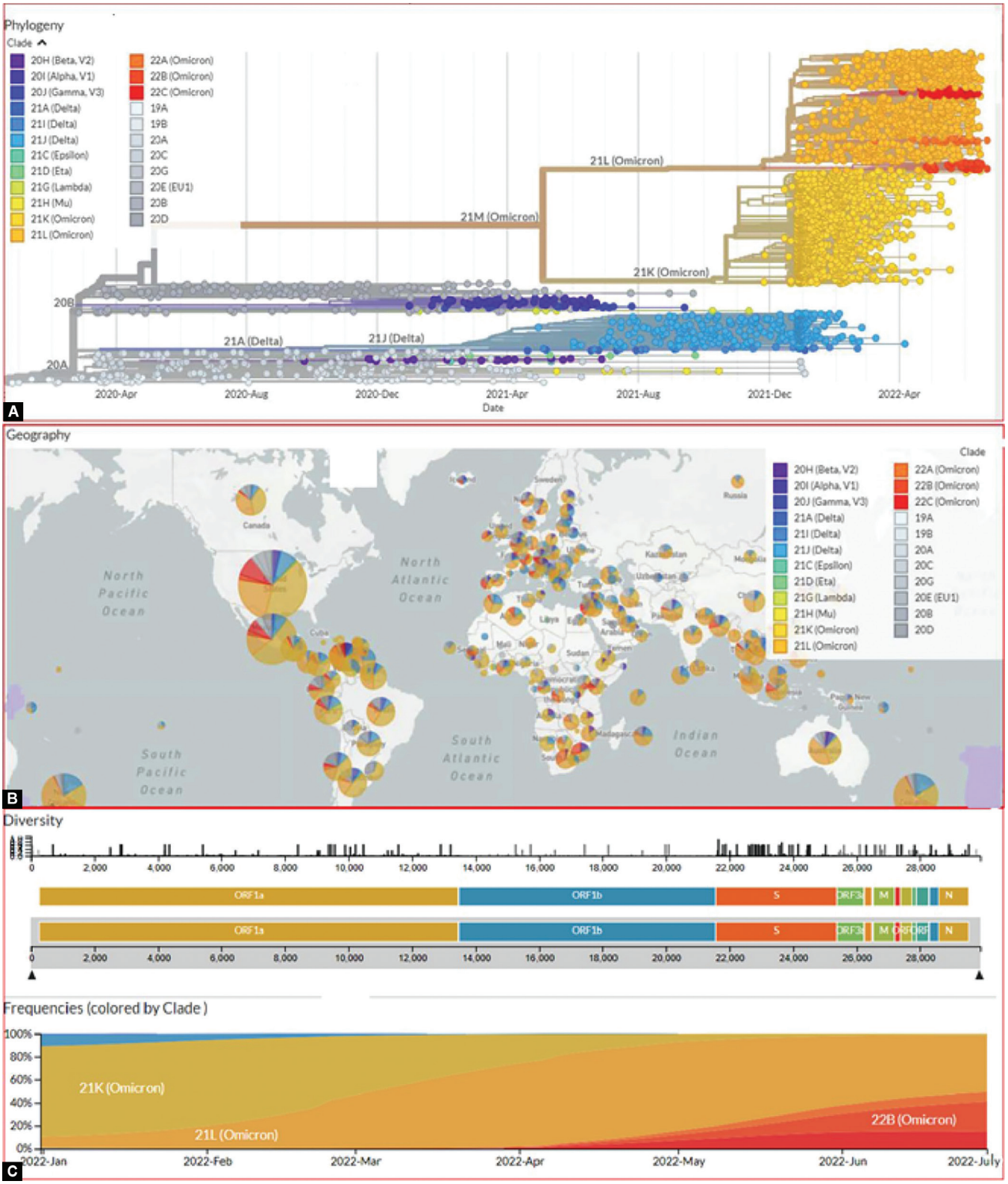

Figs 1A to C: SARS-CoV-2 genomic epidemiology with a recent six-month global subsample (A) Phylogeny; (B) Geography; (C) Diversity and frequency of COVID-19 variants based on mutations on their spike protein

Source: https://nextstrain.org/ncov/gisaid/global/6m; accessed on 28 June 2022

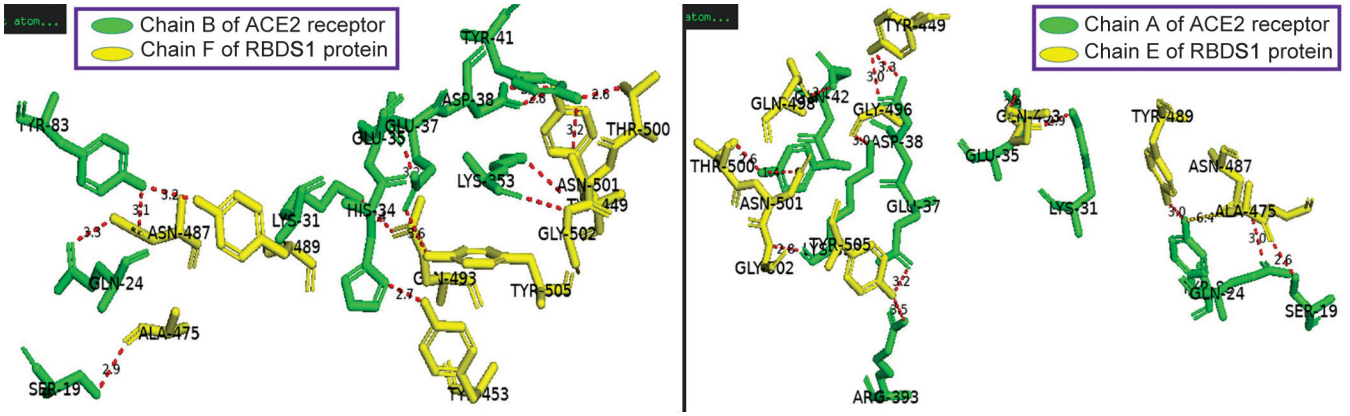

Fig. 2: SARS-CoV-2 virus and host protein interaction site

Table 1: List of RBDS1-ACE2 receptor interaction site

Chain E–Chain A interaction	*Distance*	*Chain F–Chain B interaction*	*Distance*
GLN498-TYR41	2.6	THR500-TYR41	2.6
THR500-GLN42	3.1	ASN501-TYR41	3.2
GLN493-LYS31	2.9	TYR449-LYS353	3.1
GLN493-GLU35	2.9	TYR505-GLU37	3.6
TYR489-TYR83	3	GLY502-LYS353	3
TYR505-ARG393	3.5	TYR489-TYR83	3.2
TYR505-GLU37	3.2	ASN487-TYR83	3.1
TYR449-ASP38	3.3	GLN474-GLN24	3.3
TYR449-ASP38	3	ALA475-SER19	2.9
GLY502-LYS353	2.8	GLN493-LYS31	3.4
ASN501-LYS353	3	TYR453-HIS34	2.7
ASN501-TYR41	1.4	GLN493-GLU35	3.2
ASN487-TYR83	2.9	TYR449-ASP38	2.8
GLN474-GLN24	3	------	-----
ALA475-SER19	2.6	------	-----

secondary metabolites in medicinal plants and as novel scaffolds for the creation of new drugs. Several types of secondary metabolites including triterpenes, anthocyanins, and diterpenes were isolated from *Euphorbia neriifolia* plants by different methods. Principal components have been identified including abietane, isopimarane, kaurane, and lathyrane as diterpenoids showed anti-HIV activity.[36–41] Currently, several phytochemicals from the terpenoids, alkaloids, and flavonoids families are being used to treat medical disorders such as medications, cycloartenol, euphol, neriifoliol, euphorbol, delphin, tulipanin, antiquorin and ingenol triacetate were isolated from latex, bark, root, whole plant and leaf.[36,42–46] All of these compounds are reclaimed for the aim of reducing SARS-CoV-2 pathogenesis, therefore reducing the alarming death rate.

In light of this, the current study will combine molecular docking, ADMET profiling, and molecular dynamics simulation (MDS) studies to assess the effectiveness of 17 bioactive compounds from *Euphorbia neriifolia* against the SARS-CoV-2 protein target ACE2 (PDB ID: 6VW1). This study aims to serve as a starting point for future research into specific COVID-19 treatment regimens.

Results

Structural Analysis of COVID-19-ACE2 Interaction

According to structural research, an ACE2 ligand-binding site has been discovered inside the structure of the SARS-CoV-2 spike protein (S), which acts as one of the most important drug binding sites (Fig. 2 and Table 1). Because the receptor atoms are visible in the structure, RBDS1 may be utilized to mimic stiff molecular docking.

Molecular Docking Analysis

A control drug, β-amyrin, delphin, epi-friedelanol, euphol, pelargonin, taraxterol, and tulipanin interacting with 6VW1 in a docking simulation were shown in Figure 3. As determined by the scoring function, which considers the drug binding probability to the receptor site. The CASTp online server validated that all compounds bind to the active site of the ACE2 protein receptor. Of all phytochemicals tested in Figures 4 and 5 Delphin showed the best docking score (–10.4 kcal/mol) with the SARS-COV-2 ACE2 host protein. Delphin presented six hydrogen bonds including ARG273, ASP367, SER409, HIS505 (conventional), PRO346, HIS374 (carbon) and four hydrophobic bonds interactions with LEU370 respectively. Epi-friedelanol exhibited only hydrophobic bond interaction with TRP271, PHE274 (Pi-Alkyl) and LEU144, ARG273 (Alkyl). Tulipanin showed six hydrophobic bonds interaction including TRP271, PHE274, HIS374, and ARG273 with ACE2 protein (binding affinity –9.6 kcal/mol). However, only six hydrogen bonds including GLN 102, TYR 196, GLU 208, GLY 205, and ALA 99 amino acids directly bind to the ACE2-RBDS1 receptor site. Beta-amyrin and taraxterol display hydrophobic bonds interactions with PHE274, HIS374, HIS505, TYR515, LEU370, ILE446 and TRP271, PHE274, ARG273, LEU370, respectively. and respectively, and a docking score (–10.0 and –9.4 kcal/mol). Euphol showed one hydrogen bond interaction with HIS 378 and binding affinity (–8.7 kcal/mol). Lastly, the control ligand (2-acetamido) showed three conventional hydrogen bonds including LEU370, THR371, and SER409; one hydrophobic bond HIS374. Selected 10 compounds and control ligand (2-acetamido) docking interactions were visualized and calculated in Figure 4 and Table 2, respectively.

ADMET Properties Analysis

Phytochemicals' Molecular Characteristics

The molecular properties of the phytochemicals utilized in this investigation are presented in Table 3. It was observed that

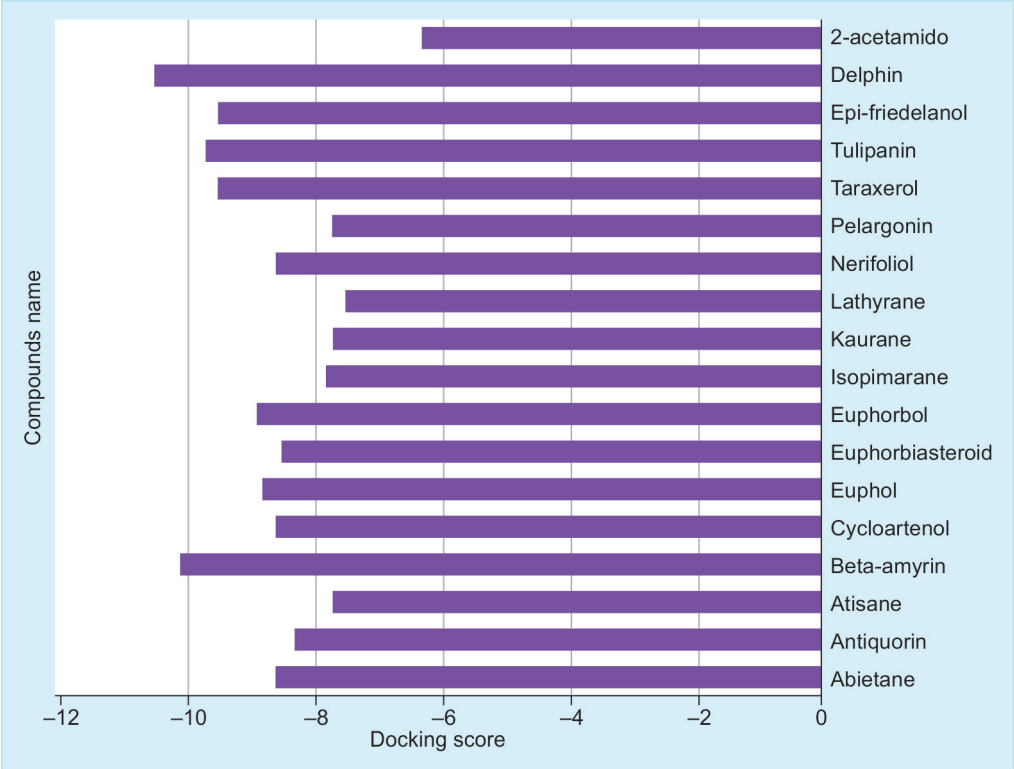

Fig. 3: Comparing binding score between our selected (A) phytochemicals and control ligand (2-acetamido)

delphin had a higher molecular weight at 627.528, followed by tulipanin at 611.529, epi-friedelanol at 428.745, and the rest of the compounds at 426.729. The highest and lowest surface area of the phytochemicals of delphin and epi-friedelanol were 246.328 and 193.088, respectively. Only delphin and tulipanin have a higher number of hydrogen bond acceptors and donors.

Phytochemical Absorption Properties Predicted

Delphin has the highest water solubility (–2.886), whereas euphol has the lowest (–7.498). However, the lowest Caco-2 permeability value was found in delphin with a value of –1.632. While delphin may not be absorbed by the intestinal cells, epi-friedelanol provides higher absorption in intestinal cells. Only delphin showed P-glycoprotein substrate activities and did not show P-glycoprotein I or II inhibitors compared to other phytochemicals (Table 4).

The Compounds' Cytochrome P450 (CYP) Promiscuity and Probable In Vivo Distribution

The estimated compound bioavailability and distribution are shown in Table 5. Tulipanin showed a higher steady-state volume of distribution than other phytochemicals that have been examined. Our study also indicates that tulipanin and delphin showed the highest unbound fraction in the blood of humans than expected results. They all have blood-brain barrier and central nervous system permeability values that are quite low. The phytochemicals that were tested for CYP promiscuity are shown in Table 6. Furthermore, none of the compounds were discovered to be CYP1A2 substrates, whereas only tulipanin and delphin were revealed to be CYP3A4 substrates. All phytochemicals are not inhibitors of the enzymes CYP1A2, CYP2C19, CYP2C9, CYP2D6, CYP3A4.

The Phytochemicals' Predicted In Vivo Clearance

The estimated clearance of each of the phytochemicals is shown in Table 7. The total clearance rate for euphol showed the highest value of 0.403 whereas delphin showed the lowest value of –0.181. For the renal organic cation transport, all phytochemicals are not substrates.

Probable Toxicological Profile of the Phytochemicals

Each of the substances examined had an expected toxicological profile, as shown in Table 8. Bacteria are not susceptible to mutagenicity of all phytochemicals (AMES toxicity). Hepatic and skin cells are not adversely affected by any of the phytochemicals. As a rule, the phytochemicals do not interfere with the hERG I (human ether-a-go-go related gene I) gene, on the other hand, all compounds may inhibit the hERG II gene. As a result, all phytochemicals have relatively low maximum tolerated dosage values except tulipanin and delphin.

Molecular Dynamic Simulation

The robustness and interactions between molecules of a protein-ligand complex are examined using real-time MD simulations. This method may be used to identify modifications in conformation that have occurred when a complex system is exposed to an artificial environment. Researchers were able to get a better understanding of the structural modifications of the molecule in the complex by using a 100 numbers Monte Carlo MD simulation of the molecule reacting to the specific receptor. The first step was analyzing the intermolecular communication behavior using the terminal samples of 100 numbers MD simulation trajectories.

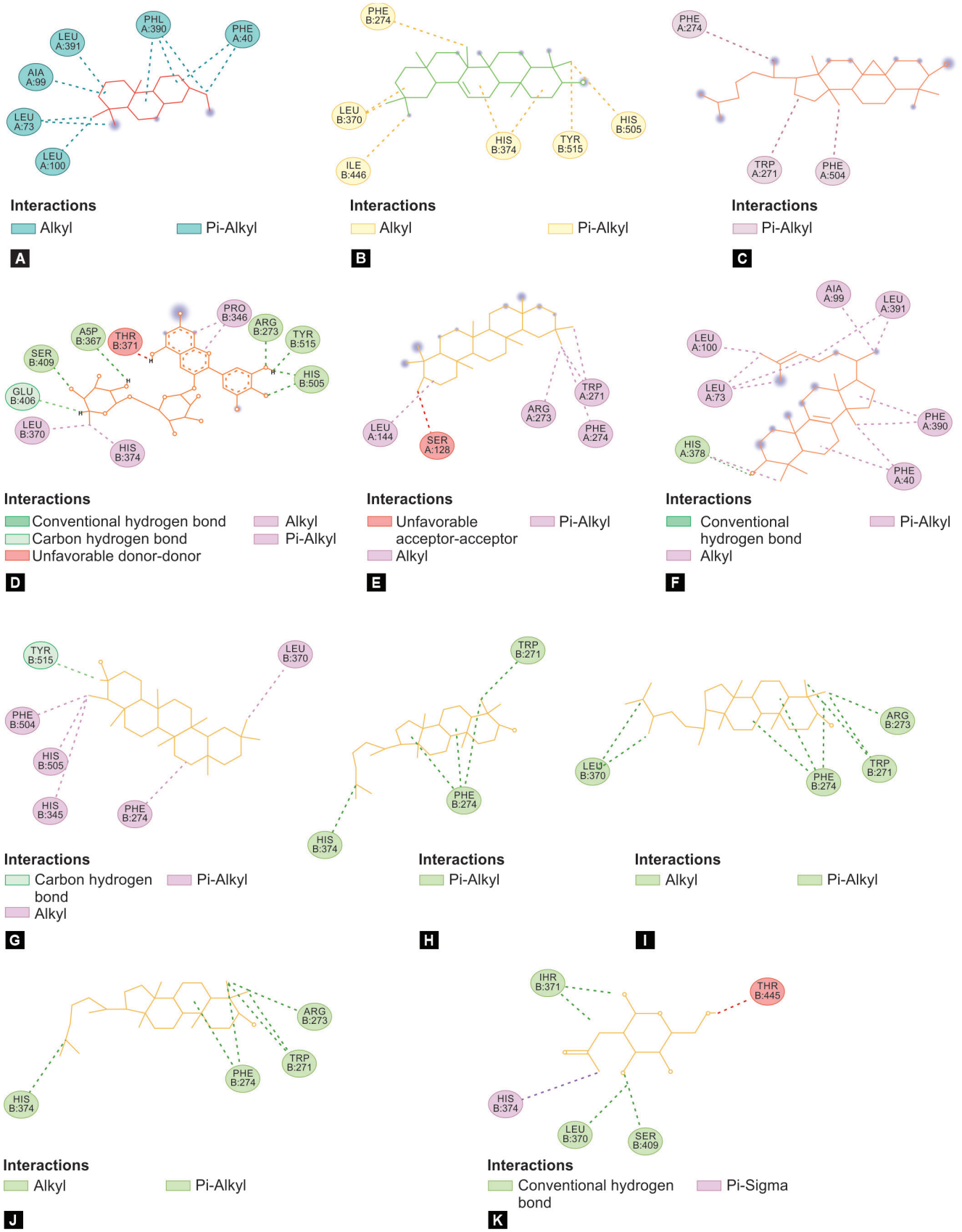

Figs 4A to K: Molecular interaction analysis of our selected 10 phytocompounds against RBDS1-ACE2 receptor protein (PDB ID: 6VW1) (A) Abietane; (B) Beta-amyrin; (C) Cycloartenol; (D) Delphin; (E) Epi-friedenalol; (F) Euphol; (G) Euphorbol; (H) Nerifoliol; (I) Taraxerol; (J) Tulipanin; (K) 2-acetamido-2-deoxy-beta-D-glucopyranose (control)

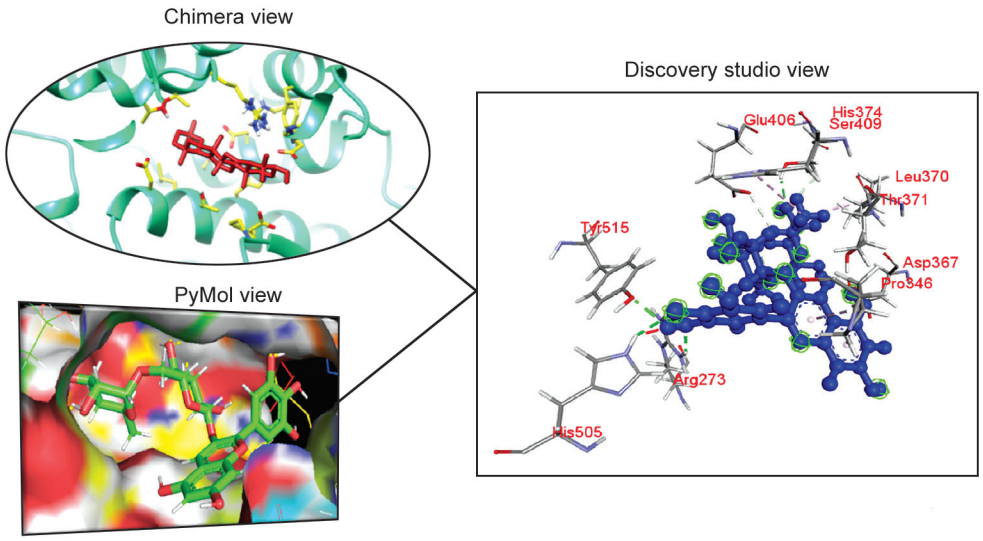

Fig. 5: Delphin showed the best docked molecule and visualized it in three structural formats. Chimera and PyMol show the 3D view, whereas discovery studio visualizer represents the 2D view

Table 2: Molecular interaction analysis of 10 selected phytocompounds and control ligand

		Amino acids				
		Hydrogen bond		*Hydrophobic bond*		
Compounds	*Docking score*	*Conventional*	*Carbon*	*Pi-Alkyl*	*Alkyl*	*Number of total bonds*
Abietane (6857485)	–8.5	–	–	ALA99, PHE40, and PHE390	LEU391, LEU100, and LEU73	10
β-amyrin (73145)	–10	–	–	PHE274, HIS374, HIS505, and TYR515	LEU370 and ILE446	8
Cycloartenol (92110)	–8.5	–	–	TRP271, PHE274, and PHE504	–	3
Delphin (10100906)	–10.4	TYR515, ASP367, ARG273, SER409, and HIS505	GLU406, and SER409	PRO346, and HIS374	LEU370	10
Epi-friedelanol (119242)	–9.4	–	–	TRP271 and PHE274	LEU144 and ARG273	6
Euphol (441678)	–8.7	HIS378	–	PHE40, HIS378, and PHE390	ALA99, LEU391, LEU73, and LEU100	13
Euphorbol (10863111)	–8.8	–	TYR515	PHE274, HIS345, PHE504, and HIS505	LEU370	6
Nerifoliol (40567592)	–8.5	–	–	TRP271, PHE274, and HIS374	–	5
Taraxerol (92097)	–9.4	–	–	TRP271 and PHE274	ARG273 and LEU370	8
Tulipanin (5492231)	–9.6	–	–	TRP271, PHE274, and HIS374	ARG273	6
2-acetamido-2-deoxy-beta-D-glucopyranose (control) (24139)	–6.2	LEU370, THR371, and SER409		HIS374 and THR445	–	5

RMSD Analysis

When determining whether or not a close-match docked position was predicted by the docking simulation, root-mean-square deviation (RMSD) values between a crystal and anticipated structures are often employed. A reasonably excellent RMSD value is one that is ≤2 Å.[47]

Target protein conformational change during interaction with three ligand molecules (β-amyrin, delphinidin, and tutupanin; CID-5492231) has to be investigated; the likelihood was calculated using MD simulations running for 100 numbers. The ligand molecule Delphin has an average RMSD of 1.5–2.5. The two ligand molecules that follow, β-amyrin and tulipanin, exhibit moderate

Table 3: Molecular properties and drug-likeness analysis of the phytochemicals

Descriptor	*Molecular weight*	*Log P*	*Rotatable bonds*	*Acceptors*	*Donors*	*Surface area*	*Lipinski rule*
Abietane	276.508	6.3013	1	0	0	126.656	Yes; 1 violation
β-amyrin	426.729	8.1689	0	1	1	192.398	Yes; 1 violation
Cycloartenol	426.729	8.1689	4	1	1	192.398	Yes; 1 violation
Euphol	426.729	8.4791	4	1	1	192.714	Yes; 1 violation
Euphorbol	440.756	8.7251	5	1	1	199.079	Yes; 1 violation
Nerifoliol	426.729	8.4791	4	1	1	8.4791	Yes; 1 violation
Taraxerol	426.729	8.1689	0	1	1	192.398	Yes; 1 violation
Tulipanin	611.529	–1.0606	6	15	11	241.533	No; 3 violation
Epi-friedelanol	428.745	8.2488	0	1	1	193.088	Yes; 1 violation
Delphin	627.528	–2.4393	7	16	12	246.328	No; 3 violation

Table 4: Predicted absorption properties of the phytochemicals

Model name	*Abietane*	*Beta-amyrin*	*Cycloartenol*	*Euphol*	*Euphorbol*	*Nerifoliol*	*Taraxerol*	*Tulipanin*	*Epi-friedelanol*	*Delphin*
Water solubility (log mol/L)	–6.735	–6.31	–5.762	–7.498	–7.576	–7.498	–6.31	–2.892	–5.572	–2.886
Caco-2 permeability (log Papp in 10–6 cm/s)	1.419	1.226	1.194	1.203	1.229	1.203	1.212	–1.274	1.22	–1.632
Intestinal absorption (human) (% Absorbed)	96.187	93.733	95.248	93.119	93.469	93.119	94.036	10.763	95.938	0
Skin permeability (log Kp)	–2.615	–2.811	–2.826	–2.926	–2.919	–2.926	–2.788	–2.735	–2.732	–2.735
P-glycoprotein substrate	No	No	No	No	No	No	No	Yes	No	Yes
P-glycoprotein I inhibitor	No	Yes	Yes	Yes	Yes	Yes	Yes	No	Yes	No
P-glycoprotein II inhibitor	Yes	Yes	Yes	Yes	Yes	Yes	Yes	Yes	Yes	No

Table 5: Predicted *in vivo* distribution of the phytochemicals

Model name	*VDss (human) (log L/kg)*	*Fraction unbound (human) (Fu)*	*BBB permeability (log BB)*	*CNS permeability (log PS)*
Abietane	0.358	0	0.868	–0.939
β-amyrin	0.268	0	0.667	–1.773
Cycloartenol	–0.075	0	0.794	–1.714
Euphol	0.66	0	0.683	–2.254
Euphorbol	0.642	0	0.734	–2.026
Nerifoliol	0.66	0	0.683	–2.254
Taraxerol	0.206	0	0.678	–1.891
Tulipanin	1.623	0.219	–2.495	–5.162
Epi-friedelanol	–0.082	0	0.7	–1.674
Delphin	0.888	0.323	–2.725	–5.508

variability in the middle of their 100 numbers simulation course, with average RMSD of 2–4 and 1.4–4, respectively. The protein-ligand complex structure seen in Figure 6 seems to be conformationally stable since the compound's fluctuation is extremely small and within allowable bounds (Table 8).

RMSF Analysis

When distinct ligand molecules link to specific residues, the root-mean-square-fluctuation (RMSF) allows us to understand and quantify the regional alterations that occur in the sequence of amino acids. As depicted in Figure 7, RMSF values were calculated for β-amyrin, delphin, and tulipanin with SARS-Cov-2 receptor

Table 6: Predicted human cytochrome P450 promiscuity of the phytochemicals

Model name	*CYP2D6 substrate*	*CYP3A4 substrate*	*CYP1A2 inhibitor*	*CYP2C19 inhibitor*	*CYP2C9 inhibitor*	*CYP2D6 inhibitor*	*CYP3A4 inhibitor*
Abietane	No	Yes	Yes	No	No	No	No
β-amyrin	No	Yes	No	No	No	No	No
Cycloartenol	No	Yes	No	No	No	No	No
Euphol	No	Yes	No	No	No	No	No
Euphorbol	No	Yes	No	No	No	No	No
Nerifoliol	No	Yes	No	No	No	No	No
Taraxerol	No	Yes	No	No	No	No	No
Tulipanin	No	No	No	No	No	No	No
Epi-friedelanol	No	Yes	No	No	No	No	No
Delphin	No	No	No	No	No	No	No

Table 7: Predicted *in vivo* clearance of the phytochemicals

Model name	*Total clearance (log mL/min/kg)*	*Renal OCT2 substrate*
Abietane	0.625	No
β-amyrin	–0.044	No
Cycloartenol	0.262	No
Euphol	0.403	No
Euphorbol	0.396	No
Nerifoliol	0.403	No
Taraxerol	–0.081	No
Tulipanin	–0.41	No
Epi-friedelanol	0.015	No
Delphin	–0.181	No

binding domain subunit 1 to analyze the change in protein architectural versatility caused by the attaching of several ligand molecules to a particular receptor site. Alpha helices and beta strands, two of the most rigid secondary structural components, were shown to have an observation rate ranging from 5 to 290 amino acid residues. There is a large amount of variation in the protein's domains at the N and C-terminal, which account for the majority of the variance. The above resulted in low fluctuation probabilities for individual atom displacement in the three ligand compounds examined.

Ligand Properties Analysis

The gyration radius (Rg), of a protein-ligand interaction system may be calculated by looking at how their individual atoms are arranged around their central axis. Calculating Rg is vital for predicting a macromolecule's structural function since it represents changes in complicated compactness over time. The effects of simulating β-amyrin delphin, and tulipanin for 100 numbers are depicted in Figure 8 along with the Rg stability of each compound in contact with the target protein. We found that the β-amyrin, delphin, and tulipanin ligand molecules had Rg values of 4.4, 5.3, and 5, respectively, indicating that binding to the protein does not significantly alter the protein's structural binding site.

The amount of solvent-accessible surface area (SASA) that biological macromolecules have impacted their organization and activity. The majority of amino acid sequences on the protein molecule can behave as binding sites or interface with other biomolecules, which helps researchers better understand the solvent-like properties of chemical compounds and their interactions with proteins.

This led to the determination of the SASA) score for the polypeptide covalently coupled to β-amyrin, delphin, and tulipanin, which is shown in Figure 8. If an amino acid residue in a complex system had a SASA value between 50 and 360 A2, it was exposed to considerable amounts of the specified ligand molecules. When using a probe radius of 1.4, the molecular surface area (MolSA) is equal to the van der Waals surface area. In silico investigation shows that the ligands β-amyrin, delphin, and tulipanin all exhibit the typical van der Waals surface area (Fig. 8). The polar surface area (PSA) of the protein-ligand interaction complexes was evaluated using the 100 numbers simulated interaction diagram. The selected three ligand compounds β-amyrin, delphin, and tulipanin were depicted in Figure 8 to show how they interacted with the chosen protein.

Analysis of Intramolecular Bonds

For a 100 numbers simulation time, the intermolecular interactions of a protein's complex structure with the provided ligands were examined using a simulation interaction diagram (SID). Hydrogen bonds, ionic bonds, noncovalent (hydrophobic), and water bridge bonds all affect protein-ligand interactions. Figure 9 depicts these interactions for (A) β-amyrin, (B) delphin, and (C) tulipanin. For all compounds, the 100 numbers simulation period resulted in multiple hydrogen, hydrophobic, ionic, and water-bridge binding connections, which were then sustained until the simulation was finished, leading to the formation of a permanent binding with the specified protein.

Binding Free Energy Calculation through MM/GBSA Analysis

Molecular Mechanics of Generalized Born and Surface (MM/GBSA) analysis was used to estimate the ligand-binding free energies to the protein receptor. The binding energies snapshots were taken from every 20 of 100 numbers simulation trajectory. The average binding energies of the complex structures are higher negative binding free energies for β-amyrin, delphin, and tulipanin are –38.5275 kcal/mol, –60.4645 kcal/mol, and –66.9365 kcal/mol respectively (Fig. 10). During the calculation, β-amyrin and delphin

Table 8: Predicted toxicological profile of the phytochemicals

Model name	*Abietane*	*β-amyrin*	*Cycloartenol*	*Euphol*	*Euphorbol*	*Nerifoliol*	*Taraxerol*	*Tulipanin*	*Epi-friedelanol*	*Delphin*
AMES toxicity	No	No	No	No	No	No	No	No	No	No
Maximum tolerated dose (human) (log mg/kg/day)	–0.754	–0.56	–0.46	–0.568	–0.275	–0.568	–0.623	0.441	–0.518	0.462
hERG I inhibitor	No	No	No	No	No	No	No	No	No	No
hERG II inhibitor	Yes	Yes	Yes	Yes	Yes	Yes	Yes	Yes	Yes	Yes
Oral rat acute toxicity (LD50) (mol/kg)	2.064	2.478	2.627	1.906	1.837	1.906	2.386	2.487	2.675	2.487
Oral rat chronic toxicity (LOAEL) (log mg/kg_bw/day)	1.394	0.873	0.806	0.788	0.786	0.788	0.808	3.465	0.883	5.069
Hepatotoxicity	No	No	No	No	No	No	No	No	No	No
Skin sensitization	No	No	No	No	No	No	No	No	No	No
T. Pyriformis toxicity (log µg/L)	0.723	0.383	0.305	0.736	0.671	0.736	0.359	0.285	0.303	0.285
Minnow toxicity (log mM)	–1.216	–1.345	–1.928	–1.757	–2.234	–1.757	–1.511	6.841	–1.78	11.071

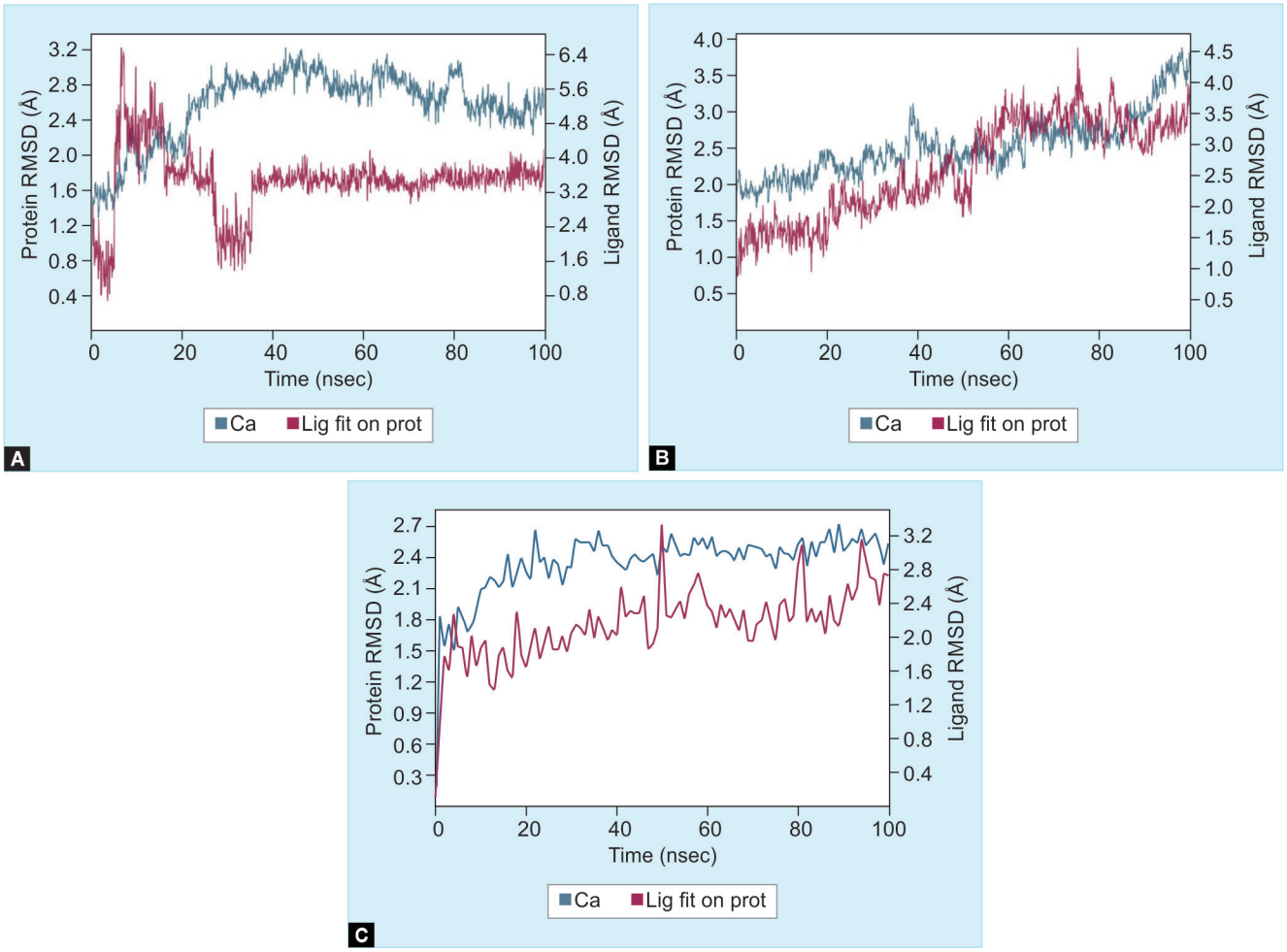

Figs 6A to C: The figure summarizes the RMSD values for the SARS-Cov-2 ACE2 protein complex with the three ligand molecules extracted from the complex system's C atoms. The selected three ligands compound (A) β-amyrin; (B) Delphin; (C) Tulipanin in interaction with the chosen protein

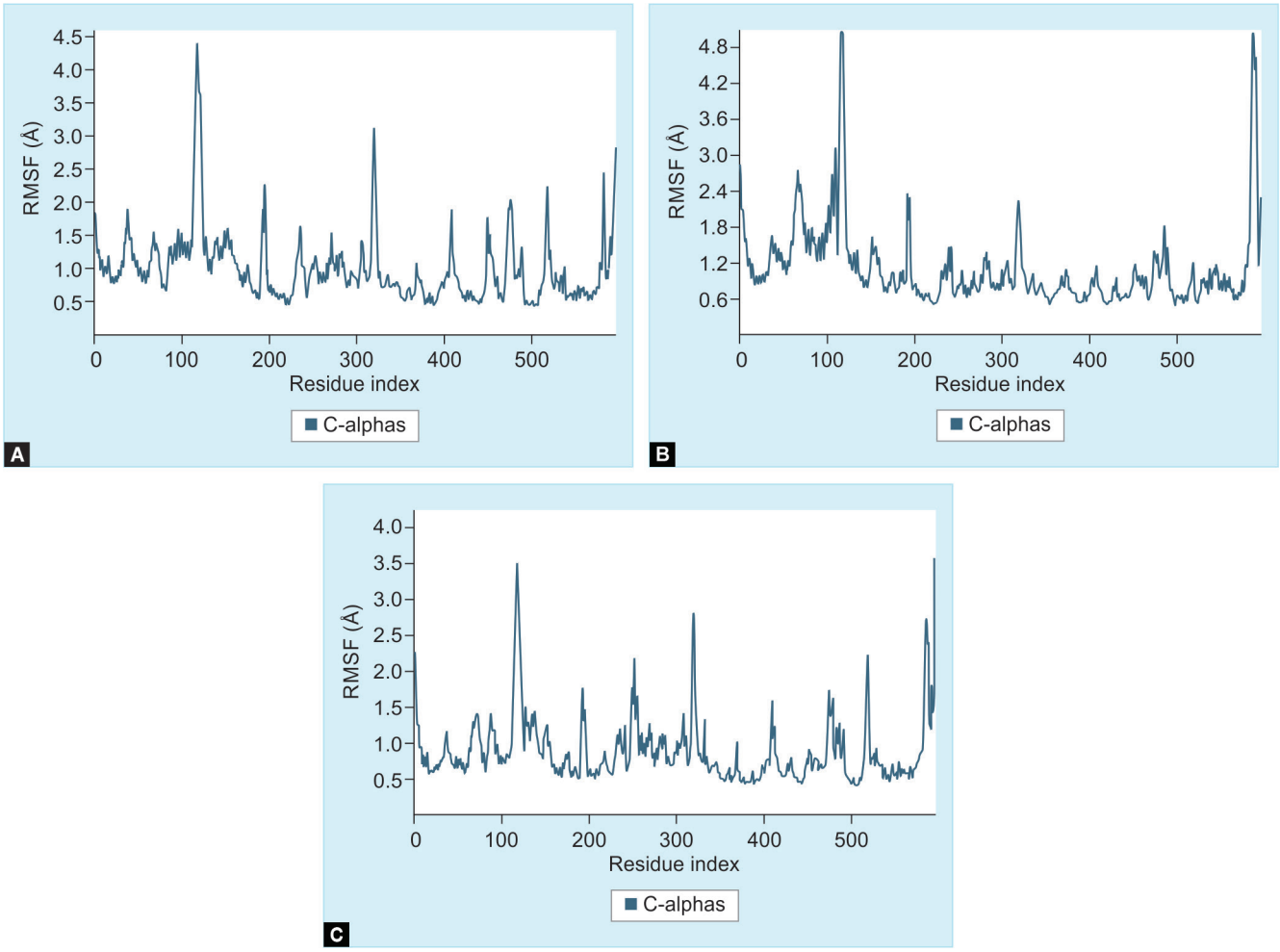

Figs 7A to C: Docked protein-ligand complexes had their RMSF values for protein C atoms measured. The selected three ligands compound (A) β-amyrin; (B) Delphin; (C) Tulipanin in interaction with the selected protein

give the exact 51 structures but tulipanin returns 6 structures over the 100 numbers trajectory, that indicates that the amyrin and delphin are maintained the convenient binding energies through the 100 numbers binding time. As a result, it is fair to suggest that the studied amyrin and delphin compounds will be capable of maintaining a long-term interaction with the targeted ACE2 receptor of the SARS-CoV-2 protein.

Discussion

Euphorbia neriifolia is a medicinal plant from the Euphorbiaceae family that has been used for millennia to control and cure a variety of infections. It is bitter, pungent, laxative, carminative, enhances appetite, beneficial in gastrointestinal problems, and causes loss of consciousness, and scientifically proven to the treatment of enlargement of the spleen, delirium, leucoderma, piles, tumors, bronchitis, anemia, ulcers, fever, cough, and asthma for being anti-inflammatory, antimicrobial and anti-parasitic properties.[33–35,48,49] The current work investigates the potential inhibitory action of specific phytochemical ingredients (β-amyrin, taraxterol, delphin, tulipanin, antiquorin, euphorbol, cycloartenol, euphol, and nerifoliol) from the *Euphorbia neriifolia* leaf extract, against the SARS-COV2 receptor protein (6VW1).

Delphin had the highest affinity for 6VW1 as revealed in the results. Our result suggests that delphin might be a potential SARS-CoV-2 inhibitor. Delphin and tulipanin are anthocyanin phytochemicals, in particular, anthocyanins, a group of photosynthetic pigments that are hydrophilic in nature. In several investigations, such as anti-Influenza virus activity, anthocyanins have been demonstrated to have antiviral properties, virus adsorption and release from infected cells were both suppressed, through generating IL-2, reducing cytokine production in the lungs and boosting T cell function.[50–52] Delphin inhibits the attachment stage, virus particles are directly affected by the entry phase.[53,54] Delphinidin-3-rutinoside, a chemical produced from the *Solanum monga* plant, inhibits HSV-1 multiplication, viral proteins, and NOX4 transcription.[55] Tulipanin, derived from the rind of *Punica granatum* Var. nana can be used as an antidiabetic agent.[56] β-amyrin, on the other hand, is a phytochemical triterpene that has been proven *in vitro* and *in vivo* to have anti-inflammatory, anti-microbial, anti-fungal, and antiviral activities.[57] According to Vitor and colleagues, suppression of NF-kB and cAMP response element binding protein (CREB) activity is most likely the principal mechanism through which triterpenes exercise their anti-inflammatory effects.[58] Holanda Pinto et al. found that β-amyrin from *Protium heptaphyllum* reduces neutrophil infiltration, oxidative stress, and TNF-α expression in rats

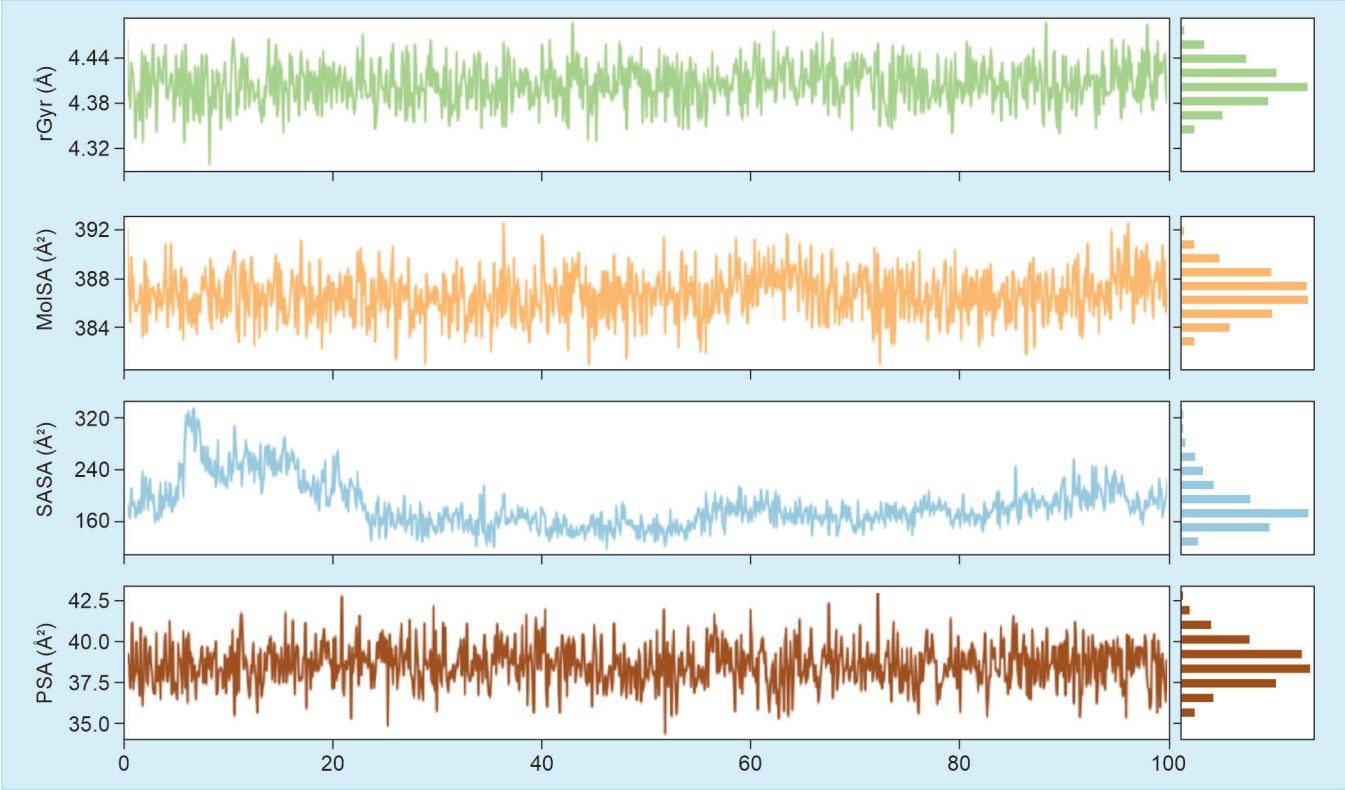

Fig. 8A: The 100 ns simulation computed the gyration radius (Rg), solvent accessible surface area (SASA), the molecular surface area (MolSA), and the polar surface area (PSA) of the beta-amyrin-protein interaction

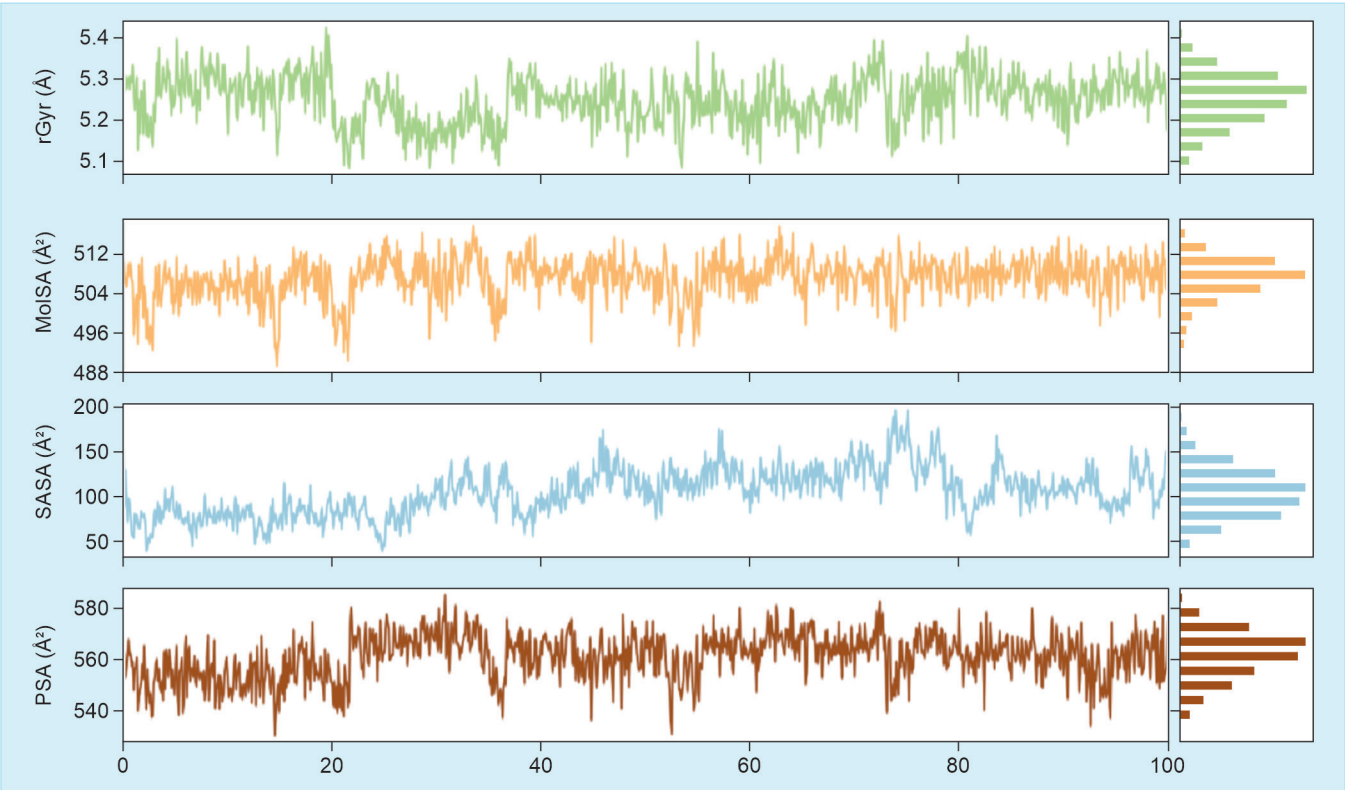

Fig. 8B: The 100 ns simulation computed the gyration radius (Rg), solvent accessible surface area (SASA), the molecular surface area (MolSA), and the polar surface area (PSA) of the delphin-protein interaction

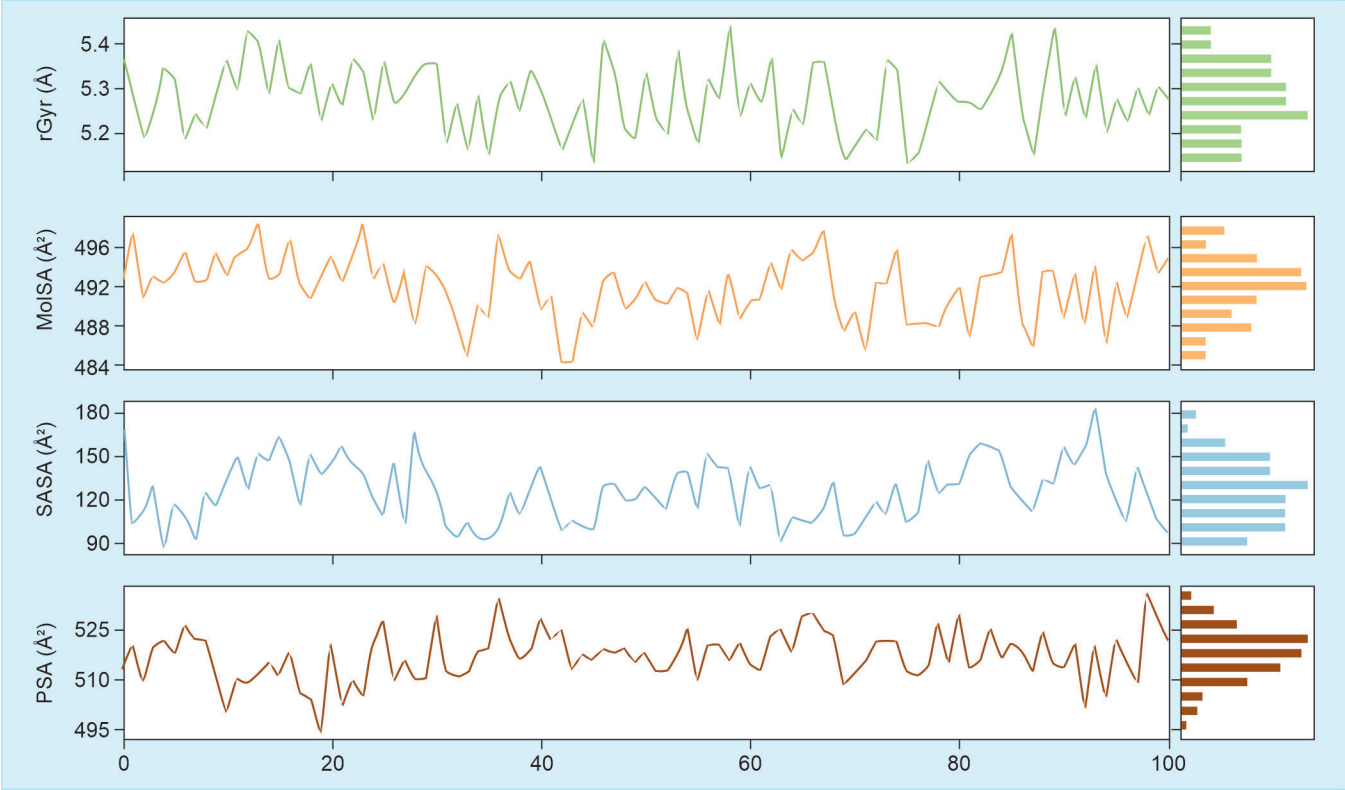

Fig. 8C: The 100 ns simulation computed the gyration radius (Rg), solvent accessible surface area (SASA), the molecular surface area (MolSA), and the polar surface area (PSA) of the tulipanin-protein interaction

in another investigation.[59] According to Jabeen et al. research, beta-amyrin has the most potent antifungal action and antimicrobial activity against the growth of some oral microbial pathogens identified by Zheng et al. studies.[60,61] The IC (50) values for beta-amyrin in the A549 and HL-60 cancer cell lines were found to be 46.2 and 38.6 M, respectively.[62] Ching et al. discovered that β-amyrin from leaf extract inhibits collagen-induced platelet aggregation more effectively than aspirin.[63] However, there exists a shortage of computational as well as clinical study information based on such medications for the treatment of SARS-CoV-2.

The ADMET profiles were evaluated as part of a systematic virtual drug and prospective drug screening can be an alternative to *in vivo* examination. The Lipinski rule is a critical criterion for identifying a molecule's pharmacological and biological activity in humans (log P).[64] Only delphin and tulipanin showed 3 violations of the Lipinski rule. The Rule of 5 states that when there are more than 5 H-bond donors, 10 H-bond acceptors, and a molecular weight of more than 500, poor absorption or penetration is more likely to occur. In general, high MW is associated with low solubility, high lipophilicity, and high metabolism rate of drug absorption that slightly affect drug-likeness properties.[11,65] Only Tulipanin and delphin were able to maintain good lipophilicity properties at appropriate concentrations in our study, which was confirmed by Hughes et al., who demonstrated that the phytochemicals have comparatively good lipophilicity as the logP values were less than five.[66] A compound is regarded to be poorly absorbed if its absorbance is lower than 30%. Only delphin showed an intestinal absorption value of zero which indicates a lower absorption rate. This is not a good sign for selecting lead compounds only in silico analysis.[67] The final bioavailability of drug candidates is calculated by digestibility and Caco-2 penetrability. For predicting the absorption of drugs taken orally, Caco-2 monolayer cells are frequently utilized as an *in vitro* model of the human intestinal mucosa. If a substance has a Papp $>8 \times 10^{-6}$, it is thought to have a high Caco-2 permeability. The tested phytochemicals (Tulipanin and Delphin) have a low Caco-2 permeability potential ($<8 \times 10^{-6}$ cm/s) and could be assimilated through the human intestine. Except for tulipanin and delphin, all phytochemicals examined were anticipated to be P-glycoprotein inhibitors, which demonstrate that they do not disrupt the typical physiological actions of P-glycoprotein (an ATP-binding cassette transporter and efflux membrane transporter found primarily in epithelial cells) which reducing active uptake and drug distribution.[68] Cytochrome P450 is a group of enzymes that play an important role in drug activation as well as drug toxicity.[68,69] Only Tulipanin and Delphin are not CYP3A4 and CYP2D6 substrates, whereas all other phytochemicals tested were either CYP2D6 or CYP3A4 substrates. The drug's lipophilicity appears to be adversely connected with metabolism-related toxicity. In addition, neither phytochemical tested was a substrate of the renal organic cation transporter, indicating they are eliminated by sweat, bile, or other mechanisms. The toxicological evaluation of the phytochemicals found that none of them are skin-toxic or hepatotoxic. Consequently, no one utilizes the AMES toxicity test to determine bacterial mutagenic potential medications. When compared to tulipanin and delphin, all compounds demonstrated a high level of toxicity in Tetrahymena pyriformis toxicity tests. However, hERG I am not inhibited by any of the phytochemicals, while all substances may inhibit hERG II. Several studies demonstrated that suppression of the hERG potassium channel might cause a delay in ventricular repolarization, disrupting the normal cardiac rhythm and causing hepatic dysfunction.[70,71]

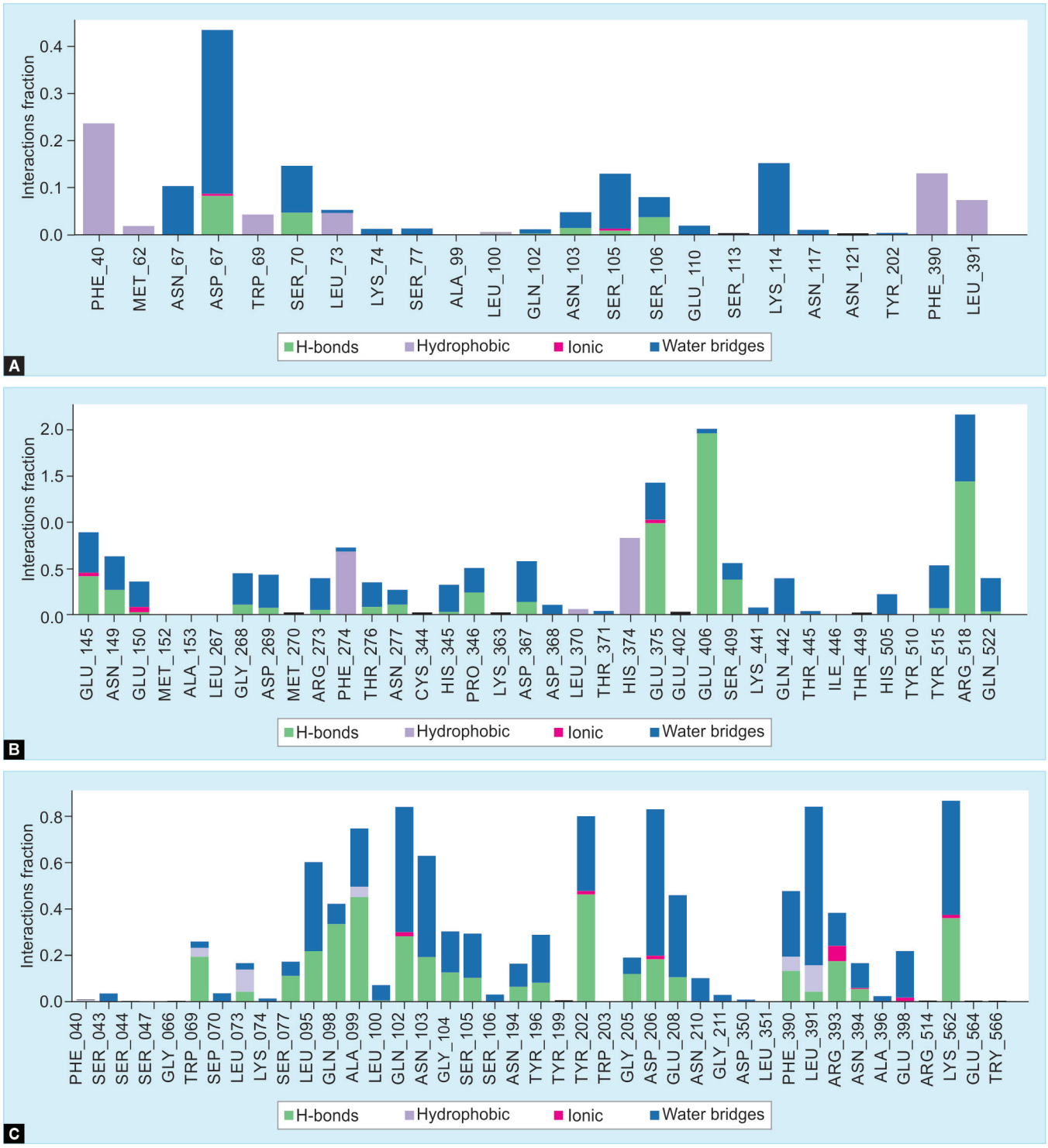

Figs 9A to C: The stacked bar chart depicts the protein-ligand interactions discovered during the 100 ns simulation. This section depicts the interactions of three different compounds. The three ligands (A) β-amyrin; (B) Delphin; (C) Tulipanin in interaction with the selected protein are shown

Molecular dynamics simulations can be used to demonstrate the consistency of a protein in a compound containing ligands.[72,73] It is also possible to measure the stiffness of protein molecules in a specific circumstance, like the human body.[72] However, the RSMF values of the protein-ligand complex are used to define the complex's mean fluctuations rather than the maximal stability of individual molecules.[74] The system RMSD was determined utilizing activities of the protein-ligand complex, which confirmed the minimum protein fluctuation. The decrease in RMSF fluctuation indicates that the molecule was stable with the target molecule. Through our research project, the compounds β-amyrin, delphin, and tulipanin had a high RMSD and RMSF value when combined with SARS-CoV-2 ACE2 protein. Baildya et al. were able to determine the molecule's rotational

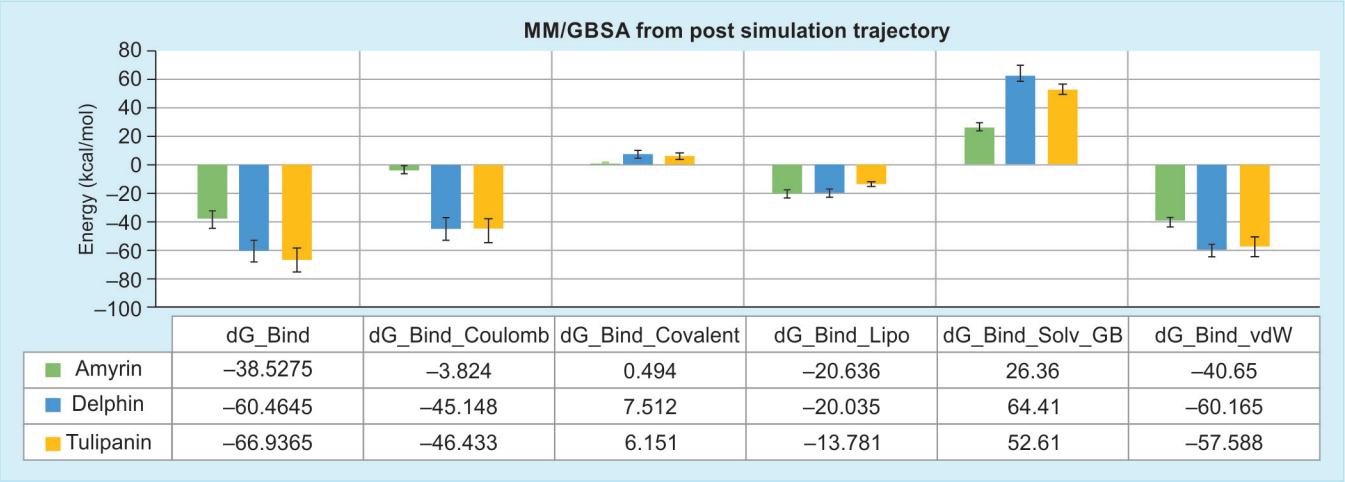

	dG_Bind	dG_Bind_Coulomb	dG_Bind_Covalent	dG_Bind_Lipo	dG_Bind_Solv_GB	dG_Bind_vdW
Amyrin	–38.5275	–3.824	0.494	–20.636	26.36	–40.65
Delphin	–60.4645	–45.148	7.512	–20.035	64.41	–60.165
Tulipanin	–66.9365	–46.433	6.151	–13.781	52.61	–57.588

Fig. 10: The calculated average binding free energies (kcal/mol) and standard deviation values of the RBDS1 of SARS-CoV-2 protein in complex with selected compounds

inertia from its C and N termini while also investigating its overall structural stability using the Rg platform.[75] Specifically, Elebeedy et al. reported that a lower Rg value implies a more compact structure, whereas a larger Rg value indicates a more dissociative structure.[76] Higher SASA values indicate that water droplets and amino acid substances have less stable structures, whereas lower SASA values indicate that water particles and amino acid residues are more compacted.[77,78] In the study, the Rg, SASA, MolSA, and PSA values of the three ligand compounds were identified to have them at their optimal levels. Furthermore, MM/GBSA values of the studied compounds will be capable of maintaining a long-term interaction with the targeted ACE2 receptor of the SARS-CoV-2 protein.

β-amyrin, delphin, and tulipanin are three ligand molecules that were chosen for the present in silico investigation, which has shown high durability against the SARS-CoV-2 ACE2 protein complex in molecular docking, ADMET profiling, and molecular dynamic simulation studies at 100 numbers time intervals. These three phytochemicals had less variation with the protein complex when RMSD and RMSF were calculated. Furthermore, these three compounds demonstrated potential outcomes in MM/GBSA, SASA, Rg, MolSA, and PSA validation. However, there is completely inadequate drug trial evidence based on these compounds for the treatment of SARS-CoV-2. Following *in vitro* and *in vivo* confirmation of anti-SARS-CoV-2 interaction, these putative pharmacologically active polyphenols could be a potential treatment strategic approach for SARS-CoV-2 therapy.

Materials and Methods

Target Preparation

The SARS-CoV-2 RBDS1 was chosen for this research based on its docking with the ACE2 protein using an X-ray structure determination (PDB ID: 6VW1). The 3D structure of the protein was downloaded from the RCSB protein data bank (http://rcsb.org). The only global repository for experimentally determined, atomically detailed three-dimensional structures of biological macromolecules, etc., was provided in the Protein Data Bank (PDB).[79] The Discovery Studio and PyMol software tools were used to remove existing ligands, oligosaccharides, chains (B, E, and F), and water molecules from the crystal structure before the docking experiments.[80,81] Then the PyMol application was also used to add hydrogen atoms that had been absent and minimized the total energy with GROMOS96 43B1 force field through SWISS PDB Viewer.[82] Active sites were predicted from raw protein through CASTp online server analysis.[83]

Ligand Preparation

We collected data on phytochemicals including β-amyrin, delphin, epi-friedenol, euphol, taraxterol, and tulipanin from the *Euphorbia neriifolia* Linn. Plant source. The phytochemical extraction processes are hydro-ethanolic, petroleum ether, benzene, chloroform, ethyl acetate, and ethanol. Ligands obtained from plant parts such as leaves, latex, stem bark, root, and fresh root were collected from the literature review.[36,84] Using the PyMol program, all substances were converted from SDF to PDB format after the molecules containing ligands were retrieved in SDF format from the PubChem database.[85–87] Next, we optimized and prepared ligands using PyRx embedded Merck Molecular Force Field (MMFF94).[88,89] The control ligand was obtained from 6VW1 PDB ID as a co-crystalized ligand.

Molecular Docking

The procedure of molecular docking has been carried out using PyRx to elucidate the connection between the medicinal molecules and the ligand.[88] The target protein's structure was considered stiff during docking, and the ligand was adaptable. The target and ligand compounds were then transformed to PDBQT format before being run. The grid settings tool has been developed using the PyRx (vina) tool grid box containing the grid box's center points (X = 102.37, Y = 0.13, Z = 159.53) and sizes (X = 69.47, Y = 72.12, Z = 61.12). We have also considered the exhaustiveness of the docking stage and it used default value 8 of PyRx software.

The ligands with the lowest RMSD values and the greatest negative docking scores were taken into consideration for ADMET evaluation. Ultimately, PyMol provided a 3D image while Discovery Studio provided a 2D representation of the docked position for molecular interactions between ligands and receptors.

ADMET Profiling

Higher binding affinity compounds like β-amyrin, delphin, epi-friedelanol, euphol, taraxterol, and tulipanin have been

chosen for the ADMET analysis. Pires et al. assessed the ADMET properties (Absorption, Distribution, Metabolism, Elimination, and Toxicological profiles) of potent drug candidates through the pkCSM tool.[90] The PubChem database provided the standard SMILE chemical structures of the compounds utilized in the investigations.[87]

Molecular Dynamic Simulation

Using 100 numbers MD simulation, the binding consistency of three potential ligand molecules—β-amyrin, delphin, and tulipanin—to the targeted SARS-Cov-2 RBDS1 with the ACE2 protein was examined (PDB ID: 6VW1).[91] The thermodynamic stability of three compounds was assessed using the "Desmond v3.6 program" from Schrodinger's (https://www.schrodinger.com/) (premium version) on an operating system based on Linux. In order to maintain a certain volume of the orthorhombic periodic boundary box shape with a mere e radius of 10 A0, the TIP3P water model was used. An appropriate ion was selected and introduced at random into the chemical solution in order to neutralize the framework.[72] The Nosé-Hoover temperature mixture and isotropic method were maintained at 300 K, one atmospheric pressure (1,01325 bar), and 50 PS capture sessions with 1.2 kcal/mol of accessible power.

Simulation Trajectory Analysis

Schrödinger Maestro, version 9.5, was used to produce all screenshots of the molecular dynamic simulation. The simulation event was analyzed and the validity of the MD simulation was established using the SID of the Desmond module in the Schrödinger suite. Utilizing trajectory performance, RMSD, RMSF, intramolecular hydrogen bonds, SASA value, Rg value, MolSA, and PSA, the sustainability of the protein-ligand complex structure was assessed.

RMSD Analysis

In molecular dynamics (MD) simulation, the RMSD represents the difference between the movement of a single atom during a specified time interval and a reference time.[72] To find the relative motion standard deviation (RMSD) of protein structural atoms like C, the side chain, the backbone, and heavier particles (in our research, 100 numbers), all time frames are aligned and compared to the reference time. The following formula can be used to evaluate the RMSD of an MD simulation with a period of x (Eq. i).

$$\mathrm{RMSD}_x = \sqrt{\frac{1}{N}\sum_{i=1}^{N}\left(\mathrm{r'i}\left(\mathrm{t_x}\right) - \mathrm{r_i}\left(\mathrm{t_{ref}}\right)\right)^2} \quad \text{(i)}$$

Here, *N* indicates the number of atoms; t_{ref} denotes the reference time; and r is the system x bit chosen after superimposing the reference system's point.

RMSF Analysis

Local variations in protein complex structure can be tracked using the RMSF.[48] The RMSF of an MD simulation of a protein with residue I may be calculated using the continuity equation (Eq. ii).

$$\mathrm{RMSF_i} = \sqrt{\frac{1}{T}\sum_{t=1}^{T} < \left(\mathrm{r'i}\left(\mathrm{t}\right) - \mathrm{r_i}\left(\mathrm{t_{ref}}\right)\right)^2 >} \quad \text{(ii)}$$

Here, *T* signifies the trajectory time in general; t_{ref} represents the reference or provided time; r refers to the position of the selected atom in framework I after transposition from the reference frame; and (< >) denotes the average square distance traversed covered over residue b.

Binding Free Energies Analysis from Post Molecular Dynamic Simulation Trajectory

The widely used molecular dynamics of generalized born and surface area (MM/GBSA) solvation technique was used to compute the liberated binding energies of ligands to the protein. The MM/GBSA binding free energy was estimated as follows: $\Delta G_{bind} = G_{complex} - G_{receptor} - G_{ligand}$, where ΔG_{bind} is the binding free energy and $G_{complex}$, $G_{receptor}$, and G_{ligand} are the free energies of complex, receptor, and ligand, respectively. The thermal MM/GBSA script provided by Schrödinger was used to calculate the ΔG_{bind} for the studied complexes.[47] The script splits the MD trajectory into individual frame snapshots and runs each one through MM/GBSA analysis. The predicted free energies (ΔG_{bind}) of binding are presented as average values.

Toxicological Research

Toxicological research is required to guarantee the safety of the use of *Euphorbia neriifolia*. OECD recommendations 420–425 guidelines were followed while determining the cytotoxicity of the saponin component of *Euphorbia neriifolia*.[92]

Conclusions

Natural products include a variety of bioactive compounds, and making them better candidates for multiple drug targets. The current work used a virtual screening strategy to identify natural phytochemicals as possible inhibitors of the SARS-CoV-2 ACE2 receptor, which is involved in viral attachment. Molecular docking to evaluate binding affinities and 100 numbers molecular dynamics analysis have been used to examine the ability of lead phytochemicals to form energetically and structurally stable complexes with the SARS-CoV-2 ACE2 protein. Because of its ability to effectively inhibit ACE2 protein, delphin (estimated binding affinity –10.4 kcal/mol) was recognized as a lead compound among the selected compounds and control drug (binding affinity –6.2 kcal/mol). Moreover, β-amyrin and tulipanin showed the ability to inhibit the ACE2 receptor with a binding affinity (–10.0 and –9.6 kcal/mol, respectively), and acceptable pharmacokinetics and physicochemical properties. Delphin is an attractive pharmaceutical option to treat COVID-19 because of its safety and minimal toxicity to normal cells, as well as its affinity and stability when forming complexes with the SARS-CoV-2 receptor protein. In-vitro investigations with delphin, β-amyrin, and tulipanin can be encouraged to identify a noble remedy for COVID-19 and to suggest a specific mechanism.

Data Availability

The data reported in this study can be found in the article. Moreover, the corresponding author may provide the reader with the data that were utilized to support the study's findings upon request.

Authors' Contributions

Conceptualization, MN Islam, MH Rahman, MS Hossen, MEA Pramanik, MMZ Miah, MJ Haque, AZM Hossain, Manzurul Islam, Mamun Mahtab, Sheikh Akbar and Ai Liang; Data curation, MEA Pramanik, MA Hossain, MA Islam, MH Rahman, MS Hossen,

MJ Haque, RA Jahan, MS Hasan, Motiur Rahman, MM Kabir, PM Basak, MR Rahman, AKMA Prodhan, Ashik Mosaddik, Humayra Haque, Fahmida Fahmin, MS Islam, HS Das, Sheikh Akbar and Ai Liang; Formal analysis, MN Islam, MEA Pramanik, MA Hossain, MA Islam, MH Rahman, MS Hossen and RA Jahan; Funding acquisition, MEA Pramanik, MMZ Miah, Istiak Ahmed, MJ Haque, AKMM Islam, MN Ali, RA Jahan, ME Haque, Munzur Rahman, MS Hasan, Motiur Rahman, MM Kabir, PM Basak, MA Sarkar, AZM Hossain, AKMA Prodhan, Ashik Mosaddik, Fahmida Fahmin, Manzurul Islam, Mamun Mahtab, Sheikh Akbar and Ai Liang; Investigation, MN Islam, MEA Pramanik, AKMM Islam, MN Ali, Munzur Rahman, MA Sarkar, AZM Hossain, MR Rahman, AKMA Prodhan, Ashik Mosaddik, MS Islam, HS Das, Humayra Haque, Manzurul Islam, Mamun Mahtab, Sheikh Akbar and Ai Liang; Methodology, MN Islam, MEA Pramanik, MA Hossain, MA Islam, MH Rahman, MS Hossen, MMZ Miah, Istiak Ahmed, MN Ali, ME Haque, MS Hasan, Motiur Rahman, MM Kabir, PM Basak, AZM Hossain, Ashik Mosaddik, Manzurul Islam, Mamun Mahtab, Sheikh Akbar and Ai Liang; Project administration, MN Islam, MEA Pramanik, Istiak Ahmed, AKMM Islam, MN Ali, RA Jahan, Chandrima Emtia, MR Gofur, AKMA Prodhan, Ashik Mosaddik, Humayra Haque, Fahmida Fahmin, Manzurul Islam, Mamun Mahtab, Sheikh Akbar and Ai Liang; Resources, MN Islam, MEA Pramanik, AKMM Islam, AZM Hossain, MR Rahman, Ashik Mosaddik, Manzurul Islam, Mamun Mahtab, Sheikh Akbar and Ai Liang; Software, MN Islam, MEA Pramanik, MH Rahman and MA Sarkar; Supervision, MEA Pramanik, Ashik Mosaddik, Manzurul Islam, Mamun Mahtab, MR Gofur, Sheikh Akbar and Ai Liang; Validation, MEA Pramanik, Ashik Mosaddik, Manzurul Islam, Sheikh Akbar and Ai Liang; Visualization, MEA Pramanik, ME Haque, Chandrima Emtia, Sheikh Akbar and Ai Liang; Writing – original draft, MN Islam, MEA Pramanik, MA Hossain, MA Islam, Motiur Rahman, MR Gofur and PM Basak; Writing – review and editing, MN Islam, MEA Pramanik, MH Rahman, MS Hossen, MMZ Miah, Istiak Ahmed, MJ Haque, AKMM Islam, MN Ali, RA Jahan, ME Haque, Munzur Rahman, MS Hasan, MM Kabir, MA Sarkar, AZM Hossain, MR Rahman, AKMA Prodhan, Ashik Mosaddik, Humayra Haque, Fahmida Fahmin, Manzurul Islam, Mamun Mahtab, Sheikh Akbar and Ai Liang. The published version of the manuscript has been read and approved by all authors.

Acknowledgments

This research is supported by ABEx Bio-Research Center, East Azampur, Dhaka 1230, Bangladesh.

Orcid

Md Enayet Ali Pramanik https://orcid.org/0000-0002-7276-331X

References

1. Zhang T, Wu Q, Zhang Z. Probable pangolin origin of SARS-CoV-2 associated with the COVID-19 outbreak. Curr Biol 2020;30(7):1346–1351.e2. DOI: 10.1016/j.cub.2020.03.022.
2. Rahman MS, Hoque MN, Islam MR, et al. Epitope-based chimeric peptide vaccine design against S, M and E proteins of SARS-CoV-2, the etiologic agent of COVID-19 pandemic: An in silico approach. Peer J 2020;8:e9572. DOI: 10.7717/peerj.9572.
3. Madjunkov M, Dviri M, Librach C. A comprehensive review of the impact of COVID-19 on human reproductive biology, assisted reproduction care and pregnancy: A Canadian perspective. J Ovarian Res 2020;13(1):140. DOI: 10.1186/s13048-020-00737-1.
4. Ciotti M, Angeletti S, Minieri M, et al. COVID-19 outbreak: An overview. Chemotherapy 2019;64(5–6):215–223. DOI: 10.1159/000507423.
5. Karim SSA, Karim QA. Omicron SARS-CoV-2 variant: A new chapter in the COVID-19 pandemic. Lancet 2021;398(10317):2126–2128. DOI: 10.1016/S0140-6736(21)02758-6.
6. Hoque MN, Akter S, Mishu ID, et al. Microbial co-infections in COVID-19: Associated microbiota and underlying mechanisms of pathogenesis. Microb Pathog 2021;156:104941. DOI: 10.1016/j.micpath.2021.104941.
7. The Nextstrain Team. Genomic epidemiology of SARS-CoV-2 with subsampling focused globally over the past 6 months. Latest global SARS-CoV-2 analysis (GISAID data). 2022. Available from: https://nextstrain.org/ncov/gisaid/global/6m.
8. Bui LT, Winters NI, Chung MI, et al. Chronic lung diseases are associated with gene expression programs favoring SARS-CoV-2 entry and severity. bioRxiv [Preprint] 2021:2020.10.20.347187. DOI: 10.1101/2020.10.20.347187.
9. Zheng Z, Peng F, Xu B, et al. Risk factors of critical & mortal COVID-19 cases: A systematic literature review and meta-analysis. J Infect 2020;81(2):e16–e25. DOI: 10.1016/j.jinf.2020.04.021.
10. Zhou F, Yu T, Du R, et al. Clinical course and risk factors for mortality of adult inpatients with COVID-19 in Wuhan, China: A retrospective cohort study. Lancet 2020;395(10229):1054–1062. DOI: 10.1016/S0140-6736(20)30566-3.
11. Machado D, Girardini M, Viveiros M, et al. Challenging the drug-likeness dogma for new drug discovery in tuberculosis. Front Microbiol 2018;9:1367. DOI: 10.3389/fmicb.2018.01367.
12. Li G, De Clercq E. Therapeutic options for the 2019 novel coronavirus (2019-nCoV). Nat Rev Drug Discov 2020;19(3):149–150. DOI: 10.1038/d41573-020-00016-0.
13. Daamen AR, Bachali P, Owen KA, et al. Comprehensive transcriptomic analysis of COVID-19 blood, lung, and airway. Sci Rep 2021;11(1):7052. DOI: 10.1038/s41598-021-86002-x.
14. Xiong Y, Liu Y, Cao L, et al. Transcriptomic characteristics of bronchoalveolar lavage fluid and peripheral blood mononuclear cells in COVID-19 patients. Emerg Microbes Infect 2020;9(1):761–770. DOI: 10.1080/22221751.2020.1747363.
15. Pramanik MEA, Miah MMZ, Ahmed I, et al. Euphorbia neriifolia leaf juice on mild and moderate COVID-19 patients: Implications in OMICRON Era. Euroasian J Hepato-Gastroenterol 2022;12(1):10–18. DOI: https://doi.org/10.5005/jp-journals-10018-1367.
16. Li S, Duan X, Li Y, et al. Differentially expressed immune response genes in COVID-19 patients based on disease severity. Aging (Albany NY) 2021;13(7):9265–9276. DOI: 10.18632/aging.202877.
17. Sungnak W, Huang N, Bécavin C, et al. SARS-CoV-2 entry factors are highly expressed in nasal epithelial cells together with innate immune genes. Nat Med 2020;26(5):681–687. DOI: 10.1038/s41591-020-0868-6.
18. Wu F, Zhao S, Yu B, et al. A new coronavirus associated with human respiratory disease in China. Nature 2020;579(7798):265–269. DOI: 10.1038/s41586-020-2008-3.
19. Hoffmann M, Kleine-Weber H, Schroeder S, et al. SARS-CoV-2 cell entry depends on ACE2 and TMPRSS2 and is blocked by a clinically proven protease inhibitor. Cell 2020;181(2):271–280.e8. DOI: 10.1016/j.cell.2020.02.052.
20. Yan R, Zhang Y, Li Y, et al. Structural basis for the recognition of SARS-CoV-2 by full-length human ACE2. Science 2020;367(6485):1444–1448. DOI: 10.1126/science.abb2762.
21. Wrobel AG, Benton DJ, Xu P, et al. SARS-CoV-2 and bat RaTG13 spike glycoprotein structures inform on virus evolution and furin-cleavage effects. Nat Struct Mol Biol 2020;27(8):763–767. DOI: 10.1038/s41594-020-0468-7.
22. Sriram K, Insel PA. A hypothesis for pathobiology and treatment of COVID-19: The centrality of ACE1/ACE2 imbalance. Br J Pharmacol 2020;177(21):4825–4844. DOI: 10.1111/bph.15082.
23. Zhang H, Penninger JM, Li Y, et al. Angiotensin-converting enzyme 2 (ACE2) as a SARS-CoV-2 receptor: Molecular mechanisms and

potential therapeutic target. Intensive Care Med 2020;46(4):586–590. DOI: 10.1007/s00134-020-05985-9.
24. Gurwitz D. Angiotensin receptor blockers as tentative SARS-CoV-2 therapeutics. Drug Dev Res 2020;81(5):537–540. DOI: 10.1002/ddr.21656.
25. Jia H, Neptune E, Cui H. Targeting ACE2 for COVID-19 therapy: Opportunities and challenges. Am J Respir Cell Mol Biol 2021;64(4):416–425. DOI: 10.1165/rcmb.2020-0322PS.
26. Dong E, Du H, Gardner L. An interactive web-based dashboard to track COVID-19 in real time. Lancet Infect Dis 2020;20(5):533–534. DOI: 10.1016/S1473-3099(20)30120-1.
27. Sohel M, Hossain M, Hasan M, et al. Management of mental health during COVID 19 pandemic: Possible strategies. Journal of Advanced Biotechnology and Experimental Therapeutics 2021;4(3):276–289. DOI: https://doi.org/10.5455/jabet.2021.d128.
28. Bhardwaj VK, Singh R, Sharma J, et al. Identification of bioactive molecules from tea plant as SARS-CoV-2 main protease inhibitors. J Biomol Struct Dyn 2021;39(10):3449–3458. DOI: 10.1080/07391102.2020.1766572.
29. Oladele JO, Oyeleke OM, Oladele OT, et al. Covid-19 treatment: Investigation on the phytochemical constituents of Vernonia amygdalina as potential Coronavirus-2 inhibitors. Comput Toxicol 2021;18:100161. DOI: 10.1016/j.comtox.2021.100161.
30. Roy S, Bhattacharyya P. Possible role of traditional medicinal plant Neem (Azadirachta indica) for the management of COVID-19 infection International Journal of Research in Pharmaceutical Sciences 2020;11(SPL1):122–125. DOI: https://doi.org/10.26452/ijrps.v11iSPL1.2256.
31. Oladele JO, Oyeleke OM, Oladele OT, et al. Kolaviron (Kolaflavanone), apigenin, fisetin as potential Coronavirus inhibitors: In silico investigation. Research Square 2020. DOI: https://doi.org/10.21203/rs.3.rs-51350/v1.
32. Ryu YB, Jeong HJ, Kim JH, et al. Biflavonoids from Torreya nucifera displaying SARS-CoV 3CL(pro) inhibition. Bioorg Med Chem 2010;18(22):7940–7947. DOI: 10.1016/j.bmc.2010.09.035.
33. Thorat BR, Bolli V. A review on euphorbia neriifolia plant. International Research Journal of Modernization in Engineering Technology and Science 2017;1(6):1723–1732. DOI: http://dx.doi.org/10.26717/BJSTR.2017.01.000523.
34. Hohmann J, Molnár J. [Euphorbiaceae diterpenes: plant toxins or promising molecules for the therapy?]. Acta Pharm Hung 2004;74(3):149–157. PMID: 16318224.
35. Betancur-Galvis LA, Morales GE, Forero JE, et al. Cytotoxic and antiviral activities of Colombian medicinal plant extracts of the Euphorbia genus. Memórias do Instituto Oswaldo Cruz 2002;97(4):541–546. DOI: https://doi.org/10.1590/s0074-02762002000400017.
36. Bigoniya P, Rana AC. A comprehensive phyto-pharmacological review of euphorbia neriifolia linn. Pharmacognosy Reviews 2008;2(4):57–66. Available from: https://www.phcogrev.com.
37. Koh LL, Ng AS, Tan GK. Structure of a diterpene from Euphorbia neriifolia. Acta Crystallographica Section C-crystal Structure Communications 1992;48(4):753–754. DOI: https://doi.org/10.1107/S0108270191011319.
38. Zhao JX, Liu CP, Qi WY, et al. Eurifoloids A-R, structurally diverse diterpenoids from Euphorbia neriifolia. J Nat Prod 2014;77(10):2224–2233. DOI: 10.1021/np5004752.
39. Yan SL, Li YH, Chen XQ, et al. Diterpenes from the stem bark of Euphorbia neriifolia and their in vitro anti-HIV activity. Phytochemistry 2018;145:40–47. DOI: 10.1016/j.phytochem.2017.10.006.
40. Raskin I, Ribnicky DM, Komarnytsky S, et al. Plants and human health in the twenty-first century. Trends Biotechnol 2002;20(12):522–531. DOI: https://doi.org/10.1016/S0167-7799(02)02080-2
41. Reddy L, Odhav B, Bhoola KD. Natural products for cancer prevention: A global perspective. Pharmacol Ther 2003;99(1):1–13. DOI: 10.1016/s0163-7258(03)00042-1.
42. Anjaneyulu V, Ramachandra R. Crystallization principles of Euphorbiaceae. Part IV: Triterpenes from the stems and leaves of E. neriilfolia. Curr Sci 1965;34:606–609. Available from: https://www.currentscience.ac.in/.
43. Mallavadhani UV, Satyanarayana KV, Mahapatra A, et al. A new tetracyclic triterpene from the latex of Euphorbia nerifolia. Nat prod Res 2004;18(1):33–37. DOI: https://doi.org/10.1080/10575630310001220 68.
44. Ilyas M, Parveen M, Amin KM. Neriifolione, a triterpene from Euphorbia neriifolia. Phytochemistry 1998;48(3):561–563. DOI: https://doi.org/10.1016/S0031-9422(98)00044-2.
45. Baslas RK, Agarwal R. Chemical investigation of some anti-cancer plants of Euphorbia genus. Indian journal of chemistry section b-organic chemistry including medicinal chemistry 1980;19(8):717–718. ISSN: 0376-4699. Available from: https://jglobal.jst.go.jp/en/detail?JGLOBAL_ID=200902009052591251.
46. Ng AS. Diterpenes from Euphorbia neriifolia. Phytochemistry 1990;29(2):662–664. DOI: https://doi.org/10.1016/0031-9422(90)85140-B.
47. Castro-Alvarez A, Costa AM, Vilarrasa J. The performance of several docking programs at reproducing protein-macrolide-like crystal structures. Molecules 2017;22(1):136. DOI: 10.3390/molecules22010136.
48. Gaur K, Rana AC, Nema RK, et al. Anti-inflammatory and analgesic activity of hydro-alcoholic leaves extract of Euphorbia neriifolia Linn. Asian J Pharm Clin Res 2009;2(1):26–28. Available from: https://www.researchgate.net/publication/228448383.
49. Kumara SM, Neeraj P, Santosh D, et al. Phytochemical and antimicrobial studies of leaf extract of Euphorbia neriifolia. Journal of Medicinal Plants Research 2011;5(24):5785–5788. Available from: http://www.academicjournals.org/JMPR.
50. Ikuta K, Mizuta K, Suzutani T. Anti-influenza virus activity of two extracts of the blackcurrant (Ribes nigrum L.) from New Zealand and Poland. Fukushima J Med Sci 2013;59(1):35–38. DOI: https://doi.org/10.5387/fms.59.35.
51. Knox YM, Hayashi K, Suzutani T, et al. Activity of anthocyanins from fruit extract of Ribes nigrum L. against influenza A and B viruses. Acta virologica 2001;45(4):209–215. PMID: 11885927.
52. Ren Z, Na L, Xu Y, et al. Dietary supplementation with lacto-wolfberry enhances the immune response and reduces pathogenesis to influenza infection in mice. J Nutr 2012;142(8):1596–1602. DOI: https://doi.org/10.3945/jn.112.159467.
53. Calland N, Dubuisson J, Rouillé Y, et al. Hepatitis C virus and natural compounds: A new antiviral approach? Viruses 2012;4(10):2197–2217. DOI: https://doi.org/10.3390/v4102197.
54. Vázquez-Calvo Á, Jiménez de Oya N, Martín-Acebes MA, et al. Antiviral properties of the natural polyphenols delphinidin and epigallocatechin gallate against the flaviviruses West Nile virus, Zika virus, and dengue virus. Front Microbiol 2017;8:1314. DOI: https://doi.org/10.3389/fmicb.2017.01314.
55. Di Sotto A, Di Giacomo S, Amatore D, et al. A polyphenol rich extract from Solanum melongena L. DR2 peel exhibits antioxidant properties and anti-herpes simplex virus type 1 activity in vitro. Molecules 2208;23(8):2066. DOI: https://doi.org/10.3390/molecules23082066.
56. El Deeb KS, Eid HH, Ali ZY, et al. Bioassay-guided fractionation and identification of antidiabetic compounds from the rind of Punica Granatum Var. nana. Nat Prod Res 2021;35(12):2103–2106. DOI: 10.1080/14786419.2019.1655411.
57. Hernández-Vázquez L, Palazón Barandela J, Navarro-Ocaña A. The pentacyclic triterpenes α, β-amyrins: A review of sources and biological activities. Chapter 23 In: Rao, Venketeshwer 487-502. Phytochemicals: A Global perspective of their role in nutrition and health. IntechOpen 2012; ISBN: 978-953-51-4317-8. DOI: https://doi.org/10.5772/27253.
58. Vitor CE, Figueiredo CP, Hara DB, et al. Therapeutic action and underlying mechanisms of a combination of two pentacyclic triterpenes, α-and β-amyrin, in a mouse model of colitis. Br J Pharmacol 2009;157(6):1034–1044. DOI: https://doi.org/10.1111/j.1476-5381.2009.00271.x.

59. Holanda Pinto SA, Pinto LM, Cunha GM, et al. Anti-inflammatory effect of α, β-Amyrin, a pentacyclic triterpene from Protium heptaphyllum in rat model of acute periodontitis. Inflammopharmacology 2008;16(1):48–52. DOI: https://doi.org/10.1007/s10787-007-1609-x.
60. Jabeen K, Javaid A, Ahmad E, et al. Antifungal compounds from Melia azedarach leaves for management of Ascochyta rabiei, the cause of chickpea blight. Nat Prod Res 2011;25(3):264–276. DOI: https://doi.org/10.1080/14786411003754298.
61. Zheng Y, Huang W, Yoo JG, et al. Antibacterial compounds from Siraitia grosvenorii leaves. Nat Prod Res 2011;25(9):890–897. DOI: https://doi.org/10.1080/14786419.2010.490212.
62. Thao NT, Hung TM, Lee MK, et al. Triterpenoids from Camellia japonica and their cytotoxic activity. Chem Pharm Bull (Tokyo) 2010;58(1):121–124. DOI: https://doi.org/10.1248/cpb.58.121.
63. Ching J, Chua TK, Chin LC, et al. Beta-amyrin from Ardisia elliptica Thunb. is more potent than aspirin in inhibiting collagen-induced platelet aggregation. Indian J Exp Biol 2010;48(3):275–279. PMID: 21046981.
64. Lipinski CA, Lombardo F, Dominy BW, et al. Experimental and computational approaches to estimate solubility and permeability in drug discovery and development settings. Advanced drug delivery reviews 1997;23(1–3):3–25. DOI: https://doi.org/10.1016/S0169-409X(96)00423-1.
65. Benet LZ, Hosey CM, Ursu O, et al. BDDCS, the Rule of 5 and drugability. Adv Drug Deliv Rev 2016;101:89–98. DOI: 10.1016/j.addr.2016.05.007.
66. Hughes JD, Blagg J, Price DA, et al. Physiochemical drug properties associated with *in vivo* toxicological outcomes. Bioorg Med Chem Lett 2008;18(17):4872–4875. DOI: https://doi.org/10.1016/j.bmcl.2008.07.071.
67. Klopman G, Stefan LR, Saiakhov RD. ADME evaluation: 2. A computer model for the prediction of intestinal absorption in humans. Eur J Pharm Sci 2002;17(4–5):253–263. DOI: https://doi.org/10.1016/s0928-0987(02)00219-1.
68. Srivalli KMR, Lakshmi PK. Overview of P-glycoprotein inhibitors: A rational outlook. Braz J Pharm Sci 2012;48(3):353–367. DOI: https://doi.org/10.1590/S1984-82502012000300002.
69. Cheng F, Yu Y, Zhou Y, et al. Insights into molecular basis of cytochrome p450 inhibitory promiscuity of compounds. J Chem Inf Model 2011;51(10);2482–2495. DOI: https://doi.org/10.1021/ci200317s.
70. Oso BJ, Oyewo EB, Oladiji AT. Influence of ethanolic extracts of dried fruit of Xylopia aethiopica (Dunal) A. Rich on haematological and biochemical parameters in healthy Wistar rats. Clinical Phytoscience 2019;5(9):1–10. DOI: https://doi.org/10.1186/s40816-019-0104-4
71. Wang H, Chiu M, Xie Z, et al. Synthetic microRNA cassette dosing: Pharmacokinetics, tissue distribution and bioactivity. Mol Pharm 2012;9(6):1638–1644. DOI: https://doi.org/10.1021/mp2006483.
72. Bharadwaj S, Dubey A, Yadava U, et al. Exploration of natural compounds with anti-SARS-CoV-2 activity via inhibition of SARS-CoV-2 Mpro. Brief Bioinform 2021;22(2):1361–1377. DOI: https://doi.org/10.1093/bib/bbaa382.
73. Aljahdali MO, Molla MH, Ahammad F. Compounds identified from marine mangrove plant (Avicennia Alba) as potential antiviral drug candidates against WDSV, an in-silico approach. Mar Drugs 2021;19(5):253. DOI: https://doi.org/10.3390/md19050253.
74. Krupanidhi S, Abraham Peele K, Venkateswarulu TC, et al. Screening of phytochemical compounds of Tinospora cordifolia for their inhibitory activity on SARS-CoV-2: An in silico study. J Biomol Struct Dyn 2021;39(15):5799–5803. DOI: 10.1080/07391102.2020.1787226.
75. Baildya N, Khan AA, Ghosh NN, et al. Screening of potential drug from Azadirachta Indica (Neem) extracts for SARS-CoV-2: An insight from molecular docking and MD-simulation studies. J Mol Struct 2021;1227:129390. DOI: https://doi.org/10.1016/j.molstruc.2020.129390.
76. Elebeedy D, Elkhatib WF, Kandeil A, et al. Anti-SARS-CoV-2 activities of tanshinone IIA, carnosic acid, rosmarinic acid, salvianolic acid, baicalein, and glycyrrhetinic acid between computational and in vitro insights. RSC advances 2021;11(47):29267–29286. DOI: https://doi.org/10.1039/d1ra05268c.
77. Mahmud S, Rahman E, Nain Z, et al. Computational discovery of plant-based inhibitors against human carbonic anhydrase IX and molecular dynamics simulation. J Biomol Struct Dyn 2021;39(8):2754–2770. DOI: 10.1080/07391102.2020.1753579.
78. Mahmoud A, Mostafa A, Al-Karmalawy AA, et al. Telaprevir is a potential drug for repurposing against SARS-CoV-2: Computational and in vitro studies. Heliyon 2021;7(9):e07962. DOI: https://doi.org/10.1016/j.heliyon.2021.e07962.
79. Shang J, Gang Ye, Ke S, et al. Structural basis of receptor recognition by SARS-CoV-2. Nature 2020;581(7807):221–224. DOI: https://doi.org/10.1038/s41586-020-2179-y.
80. Studio D. Dassault systems. BIOVIA Discovery Studio modelling environment, Release 4.5. Accelrys Softw Inc. 2015; 98–104. Available from: https://www.3ds.com/products/biovia/discovery-studio.
81. Schrödinger LL. The PyMOL Molecular Graphics System, Version. 2020; 2.4. Available from: https://www.scirp.org/reference/ReferencesPapers?ReferenceID=1571978.
82. Kaplan W, Littlejohn TG. Swiss-PDB viewer (Deep View). Brief Bioinform 2001;2(2):195–197. DOI: 10.1093/bib/2.2.195.
83. Tian W, Chen C, Lei X, et al. CASTp 3.0: computed atlas of surface topography of proteins. Nucleic Acids Res 2018;46(W1):W363–W367. DOI: 10.1093/nar/gky473.
84. Chang FR, Yen CT, Ei-Shazly M, et al. Anti-human coronavirus (anti-HCoV) triterpenoids from the leaves of Euphorbia neriifolia. Nat Prod Commun 2012;7(11):1415–1417. PMID: 23285797.
85. Li JC, Dai WF, Liu D, et al. Bioactive ent-isopimarane diterpenoids from Euphorbia neriifolia. Phytochemistry 2020;175:112373. DOI: 10.1016/j.phytochem.2020.112373.
86. Yuan S, Chan HCS, Zhenquan Hu. Using PyMOL as a platform for computational drug design. Wiley Interdisciplinary Reviews: Computational Molecular Science 2017;7(2):e1298. DOI: https://doi.org/10.1002/wcms.1298.
87. Kim S, Chen J, Cheng T, et al. PubChem 2019 update: Improved access to chemical data. Nucleic Acids Res 2019;47(D1):D1102–D1109. DOI: 10.1093/nar/gky1033.
88. Dallakyan S, Olson AJ. Small-molecule library screening by docking with PyRx. Methods Mol Biol 2015;1263:243–250. DOI: 10.1007/978-1-4939-2269-7_19.
89. Halgren TA. Merck molecular force field. III. Molecular geometries and vibrational frequencies for MMFF94. Journal of computational chemistry 1996;17(5-6):553–586. DOI: https://doi.org/10.1002/(SICI)1096-987X(199604)17:5/6<553::AID-JCC3>3.0.CO;2-T.
90. Pires DE, Blundell TL, Ascher DB. pkCSM: Predicting small-molecule pharmacokinetic and toxicity properties using graph-based signatures. J med chem 2015;58(9):4066–4072. DOI: https://doi.org/10.1021/acs.jmedchem.5b00104.
91. Hoffman JM, Margolis KG. Building community in the gut: A role for mucosal serotonin. Nat Rev Gastroenterol Hepatol 2020;17(1):6–8. DOI: https://doi.org/10.1038/s41575-019-0227-6.
92. Bigoniya P, Rana AC. Protective effect of Euphorbia neriifolia saponin fraction on CCl4-induced acute hepatotoxicity. African Journal of Biotechnology 2010;9(42):7148–7156. DOI: 10.5897/AJB09.1440.